ASSESSMENT OF INDOOR RADON CONCENTRATIONS AND EXPOSURE DOSE IN SELECTED OCCUPATIONAL BUILDINGS AND DWELLINGS IN KAMPALA CAPITAL CITY AUTHORITY, UGANDA

BY

SSIKUBWABO IVAN

21/U/GMSP/14627/PE

A DISSERTATION SUBMITTED TO THE DIRECTORATE OF RESEARCH AND GRADUATE TRAINING IN PARTIAL FULFILMENT OF THE REQUIREMENTS FOR THE AWARD OF THE DEGREE OF MASTER OF SCIENCE IN PHYSICS OF KYAMBOGO UNIVERSITY

SEPTEMBER, 2025

DECLARATION

I, Ssikubwabo Ivan, hereby affirm that this dissertation is a genuine account of my independent research and has not been presented to any university or institution for the purpose of obtaining an academic qualification.

Signature……………….……..……Date………..……………………………

APPROVAL

This is to certify that this research dissertation entitled “Assessment of indoor radon concentrations and exposure dose in selected occupational buildings and dwellings in Kampala City Authority, Uganda” has been written under our supervision.

Dr. Farooq Kyeyune

Signature…… ………..…..Date………09/09/2025…...……

Dr. Thomas Baluku

Signature……………………………..Date…………….………………..

ACKNOWLEDGEMENT

I am deeply thankful to the Almighty for His unwavering guidance throughout this journey. I wholeheartedly acknowledge that without His divine support, the completion of this research would not have been possible.

I extend my profound gratitude to my supervisors, Dr. Farooq Kyeyune and Dr. Thomas Baluku of Kyambogo University, whose insightful guidance and constructive feedback played a vital role in the successful completion of this study.

I am also sincerely appreciative of the management teams of the various buildings and dwellings who graciously permitted data collection under their oversight. My thanks go to all individuals who offered assistance during the data gathering process. I am especially grateful to Mr. Evarist R.S. Turyahabwe for his valuable advice and support throughout the research period.

It is with great pleasure that I acknowledge my sponsor, Joseph, for his generous financial contribution towards my education, extended through Mrs. Erina Nakamya. Lastly, I offer heartfelt thanks to my dear mother for her unwavering love, encouragement, and support particularly during the more demanding phases of data collection.

TABLE OF CONTENTS

DECLARATION ii

APPROVAL iii

ACKNOWLEDGEMENT iv

TABLE OF CONTENTS v

LIST OF FIGURES..viii

LIST OF TABLES..ix

ABSTRACT...xi

CHAPTER ONE: INTRODUCTION...1

1.1 Study background 1

1.2 Research problem tatement 2

1.3 Study objectives 4

1.3.1 General objective...4

1.3.2 Specific Objectives..4

1.4 Study significance 4

1.5 Scope and limitations 5

1.6 Dissertation structure 5

CHAPTER TWO: LITERATURE REVIEW...................................7

2.1 Overview 7

2.2 Process of radioactive decay 7

2.2.1 Alpha decay...8

2.2.2 Beta Decay 9

2.2.3 Gamma Decay 9

2.3 Environment Radiation 10

2.3.1 Ionising radiation.. 12

2.3.2 Non-ionising radiations 13

2.4 Radon in rocks and soil 13

2.5 Radon mitgration.. 14

2.5.1 Radon entry into buildings 16

2.6 Radon dose rates 18

2.7 Health risks from radon exposure 19

2.8 Comparision of indoor radon regulations and health impacts 21

2.9 Radon detection methods 22

CHAPTER THREE: MATERIALS AND METHODOLOGY 24

3.1 Overview 24

3.2 Geological scope 24

3.3 Radon activity concentration measurements.. 26

3.4 Dose estimation and risk assessment 28

3.4.1 Computation of annual effective dose (ED)... 28

3.4.2 Estimating annual equivalent dose and lifetime cancer risk (LCC).... 28

3.5. Data analysis and statistical methods.. 29

CHAPTER FOUR: RESULTS AND DISCUSSION...................................... 30

4.1 Overview 30

4.2 Mean radon concentration levels in occupational buildings 30

4.3 Activity levels of ^{222}Rn concentration in dwellings 35

4.4 Comparative analysis of indoor ^{222} Rn levels with other studies 37

4.5 Exposure dose estimation 41

4.5.1 Annual effective radiation dose for workers 41

4.5.2 Annual effective radiation dose for Dwellers 43

4.6 Excess lifetime cancer risk (ELCR) and lung cancer cases per million persons per year 44

CHAPTER FIVE: CONCLUSIONS AND RECOMMENDATIONS 46

5.0 Overview 46

5.1 Conclusion 46

5.2 Recommendation 47

REFERENCES 49

APPENDIX: RAW DATA 57

LIST OF FIGURES

Figure 2.1: Uranium decay chain..12

Figure 2.2: Spectrum of ionising radiation by wavelengths. 13

Figure 2.3: Pathways of radon migration through soil environment..................15

Figure 2.4: Pathways for ^{222} Rn infiltration into indoor air. 17

Figure 2.5: Pathway of ^{222} Rn and its decay products into the lungs...................20

Figure 3.1: Map of Kampala Capital City Authority highlighting the study locations. 25

Figure 3.2: (a) Set-up of Radon Sentinel Monitor (model 1030), and (b) Radon sentinel Detector. 26

Figure 3. 3: Illustrative layout of a radon sentinel monitoring device..................27

Figure 4.1: ^{222} Rn levels by floor: (a) basements, (b) ground floor, (c) first floor, and (d) second floor. 32

Figure 4.2: Structure cracks observed in measured workspaces. 34

Figure 4.3: Average ^{222} Rn levels across levels in poorly ventilated workplaces.34

Figure 4.4: ^{222} Rn levels in bedrooms and sitting rooms of selected dwelling buildings...36

Figure 4.5: Annual ED dose exposure for workers at different levels in different buildings...42

Figure 4.6: Annual effective radiation dose for dwellers across different dwellings. 43

LIST OF TABLES

Table 2.1: Natural decay series and half-lives (Obid et al., 2011). 11

Table 2.2: Recommended indoor ^{222} Rn concentration levels (Catão et al., 2022; Lorenzo et al., 2019). 22

Table 2.3: Common of radon detection and their features (Pantelić et al., 2019). 23

Table 4.1: Indoor ^{222}Rn concentration across various floors in occupational buildings. 31

Table 4.2: Mean values of ^{222} Rn levels in selected dwellings. 35

Table 4.3: Comparative assessment of indoor ^{222}Rn levels across various workplaces and dwellings in relation to other studies 38

Table A 1: Details about the rooms studied in the work buildings. 57

Table A 2: Details about the rooms studied in the dwellings. 60

Table B 1: Measured levels of ^{222} Rn in the basement areas of the surveyed buildings. 63

Table B 2: Measured levels of ^{222} Rn on the ground floors of the surveyed buildings. 64

Table B 3: Measured levels of ^{222} Rn on the first floors of the surveyed buildings. 65

Table B 4: Measured levels of ^{222} Rn on the second floors of the surveyed buildings. 66

Table B 5: Measured levels of ^{222} Rn in the poorly ventilated storage rooms of NK-1 building. 67

Table C 1: Measured levels of ^{222} Rn in the bedrooms of the dwellings. 68

Table C 2: Measured levels of ^{222} Rn in the sittings of the surveyed dwellings..69

Table D 1: Annual radiation effective dose, ERD, ELCR and LCC to workers ..70

Table D 2: Annual radiation effective dose, ERD, ELCR and LCC to dweller ...72

ABSTRACT

Radon exposure is recognised as a serious public health issue resulting from its pronounced effect association with lung cancer, especially in enclosed environments where its concentration can rise significantly. While much of the existing research has concentrated on radon levels in dwelling settings, there is a noticeable gap in studies examining radon exposure in workplaces particularly in fast-developing urban centres like Kampala Capital City Authority. This research aimed to bridge that gap by investigating radon dose levels and assessing the potential radiological risks faced by both employees and inhabitants in selected occupational and dwelling structures located within five administrative divisions of Kampala Capital City Authority. To achieve this, radon levels were monitored at 20 different sites comprising 10 workplaces and 10 dwellings using the Radon Sentinel Model 1030, a continuous radon monitoring instrument. ^{222}Rn levels measured in occupational structures varied between 8.7 ± 1.5 to 95.8 ± 8.0 Bq/m^3, with a mean concentration of 30.8 ± 4.5 Bq/m^3. Significantly elevated readings were observed in storage zones with limited ventilation, where values exceeded the WHO's recommended ceiling of 100 Bq/m^3, reaching a maximum of 194.8 ± 21.2 Bq/m^3. In residential buildings, ^{222} Rn levels spanned from 15.3 ± 2.3 to 188.2 ± 8.2 Bq/m^3, with an average of 71.7 ± 17.5 Bq/m^3. Several household measurements surpassed the WHO reference threshold. The corresponding annual ED estimates were 0.32 ± 0.05 mSv/year for occupational environments and 0.75 ± 0.18 mSv/year for dwelling settings—both remaining within the internationally endorsed public exposure limit of 1.0 mSv/year. Additional radiological parameters were analysed including the annual equivalent dose to lung tissue, the calculated excess lifetime risk of cancer, and the projected number of LCC attributable to ^{222} Rn exposure. Overall, the indoor ^{222} Rn concentrations recorded across the surveyed sites were relatively moderate and are not expected to present substantial health risks. Nevertheless, routine monitoring is advised to account for seasonal fluctuations and maintain long-term radiological safety for occupants of the building.

CHAPTER ONE: INTRODUCTION

1.1 Study background

Natural sources account for nearly 98% of human exposure to radiation, with approximately 52% stemming from the uranium-238 (^{238}U) decay chain (Shahbazi et al., 2013).Radon a gas that lacks taste, color, and odor is one of the radioactive byproducts of ^{238}U. Due to its non-reactive nature, radon has the ability to move freely through rocks and soil, allowing it to disperse into nearby surroundings (Muhammad et al., 2022).

Radon exists in three principal isotopic forms: ^{219}Rn, known as actinon; ^{220}Rn, referred to as thoron; and ^{222}Rn, commonly identified simply as radon. Each isotope exhibits radioactivity, with ^{222}Rn having a half-life of 3.82 days, ^{220}Rn decaying within 56 seconds, and ^{219}Rn breaking down in just 4 seconds (Tezcan et al., 2023). Since radon takes only a few minutes to move from underground into the atmosphere or indoor spaces, radon-222 (^{222}Rn) plays the most prominent role in overall radon exposure. ^{222}Rn carries no electrical charge and has a relatively long half-life, meaning most inhaled radon is exhaled before it decays and thus poses minimal direct harm. However, its decay products such as , polonium-214 (^{214}Po), polonium-218 (^{218}Po), bismuth-214 (^{214}Bi) and lead-214 (^{214}Pb) carry electrical charges and produce potent alpha particles (Lorenzo et al. 2019). These particles readily attach to airborne dust and smoke indoors.

While radon levels outdoors are typically low (Appleton et al., 2007), they can build up in enclosed environments like buildings and mines due to poor air circulation. Indoor radon levels vary based on factors including soil permeability, building design and ventilation, geological conditions, and the type of flooring materials (Kazwini et al., 2020). Radium-226 found in soil, rock, construction materials, and tap water is the major source of indoor radon. Materials like cement, bricks, and concrete generally contribute less radon due to their lower radium content compared to natural soils and rocks (Appleton et al. 2020).

Since the byproducts of radon decay have brief half-lives, they typically break down before they can travel to internal organs such as the liver or kidneys. The primary health concern from indoor radon exposure is lung cancer, caused by DNA damage in lung cells (Kpordzro et al. 2022; Trassierra et al. 2016). Studies show that indoor radon levels exceeding 100 Bq/m^3 per WHO guidelines are th leading non-tobacco-related source of lung cancer incidence (Lorenzo et al. 2019).

Although numerous countries have implemented safety guidelines and regulatory frameworks to control indoor ^{222}Rn levels, Uganda lacks both comprehensive studies and formal guidelines for residential and occupational settings. Kampala, with an estimated population of 1.9 million in 2024 (UBOS), has around 60% of its residents in the workforce (Mukwaya et.al., 2025). This population may be at risk if radon exposure surpasses internationally accepted safety limits (Muhammad et al., 2022).

Hence, this study aims to assessing indoor ^{222}Rn levels and exposure risks in selected workplaces and dwellings within Kampala City Authority to better understand radon prevalence in Uganda's indoor environments.

1.2 Research problem tatement

According to the World Health Organisation (WHO), exposure to elevated radon levels is the second leading cause of lung cancer after smoking (Muhammad et al

2022). Radon is a radioactive gas formed through natural processes, capable of entering and building up within enclosed spaces, where it may present significant health hazards, particularly in poorly ventilated spaces. In Kampala City Authority, the rapid urbanisation has led to diverse building characteristics, including a mix of modern high-rise structures and older dwellings with limited ventilation and varying construction materials. Many dwellings and occupational buildings are constructed with locally sourced materials such as fired bricks and concrete, which may contribute to radon emission (Kazwini et al., 2020). Furthermore, inadequate building codes, low awareness, and poor ventilation systems worsen the accumulation of radon indoors, especially in basements and ground floors.

Despite these risk factors, a significant data gap exists regarding indoor concentrations of ^{222}Rn and their associated radiological health risks within the Kampala region. particularly in occupational environments. While previous research has mainly focused on dwellings, limited attention has been given to workplaces where individuals remain for extended durations. Therefore, this study seeks to determine indoor radon concentrations and estimate the corresponding exposure doses in selected occupational facilities and dwelling structures across Kampala Capital City Authority. The findings are intended to facilitate the creation of a detailed radon hazard map and guide strategic public health interventions aimed at lowering the incidence of lung cancer linked to indoor radon exposure across the region.

1.3 Study objectives

1.3.1 General objective

To assess radon exposure levels and potential radiological risks for individuals in selected occupational and dwelling buildings within Kampala Capital City Authority.

1.3.2 Specific Objectives

The specific objectives of the study are to:

i. To determine and evaluate ^{222}Rn concentrations and their spatial distribution within occupational buildings and dwellings located in Kampala Capital City Authority.

ii. To calculate the ^{222}Rn exposure dose for individuals working or living in these selected buildings.

1.4 Study significance

This research will enhance public understanding of radon-related health risks, encouraging individuals to monitor radon levels and adopt safety measures in homes and workplaces. It aligns with Kyambogo University's research focus on radiation and environmental health. By contributing to Sustainable Development Goal 3 focuses on advancing health and enhancing overall well-being for individuals across all age groups. The study supports the university's mission to improve public health through targeted research. The findings will offer critical insights into ^{222}Rn exposure levels and help shape policies and building standards for radon mitigation. Additionally, the study will raise awareness about the dangers of elevated radon levels and promote proactive health protection.

1.5 Scope and limitations

This study involved measuring the ^{222}Rn levels and assessing exposure risks in 10 occupational buildings and 10 dwellings randomly selected across Kampala's five administrative divisions: Nakawa, Makindye, Rubaga, Central, and Kawempe. Data collection occurred between June 2023 and June 2024 using the Radon Sentinel Model 1030. Data collection was conducted in two to three rooms on each floor of the occupational buildings, covering areas such as basements, ground floors, and upper levels. For dwellings, measurements were obtained from rooms located at ground level, specifically bedrooms and sitting areas.

While the sample was randomly selected, it may not fully represent radon levels across Kampala due to variations in environmental and structural factors. The limited sample size and geographic coverage restrict the broader applicability of the results.

1.6 Dissertation structure

This research outlines the results of the measured indoor ^{222}Rn concetrations and the corresponding exposure doses across different occupational and dwelling buildings situated within Kampala Capital City Authority. Chapter one introduces the study by outlining its background, emphasising the importance of assessing ^{222}Rn activity concentrations, and clearly defining the research problem and objectives. Chapter Two reviews the relevant literature, situating the study within the context of previous research. Chapter Three details the methodological framework employed. Chapter Four presents the results of indoor radon measurements alongside the estimated effective doses for both workplaces and homes, followed by a discussion of the implications. Finally, Chapter Five presents the key conclusions derived from the research and outlines suggestions for future studies and policy development.

CHAPTER TWO: LITERATURE REVIEW

2.1 Overview

This chapter is divided into eight main areas This chapter is organized into eight principal sections, the process of radioactive decay, environmental sources of radiation, the occurrence of radon in geological materials, how radon moves within residential spaces, health risks linked to radon exposure, research findings on radon levels, and methods used to detect and measure radon.

2.2 Process of radioactive decay

Radioactive decay is the spontaneous decay of a nucleus, leading to the creation of a different nucleus with altered chemical properties. This transformation releases energy that comes as ionising radiation namely beta (β), alpha (α), or gamma (γ) rays (Karmaker et al. 2021).The rate at which radionuclides decay is influenced by their quantity and is unique to each isotope. This rate can be mathematically described using a first-order differential equation (2.1);

$$-\frac{dN}{dt} = \lambda N(t), \qquad (2.1)$$

Where N is the number of radionuclides at time t

By integrating this equation, we get:

$$N(t) = N_o e^{-\lambda t}, \qquad (2.2)$$

Here, N_0 represents initial quantity of radionuclides and λ represents the decay constant.

This indicates that the quantity of original nuclei and the speed at which they decay both diminish following an exponential pattern over time. The idea of half-life, denoted as $(t_{1/2})$, represents the duration needed for half of the radioactive material to experience decay

$$N(t) = N_o \left(\frac{1}{2}\right)^r, \quad (2.3)$$

The half-life ($t_{1/2}$) and decay constant (λ) are linked by the relation indicated in Equation (2.4)

$$\lambda = \frac{\ln 2}{t_{1/2}} = \frac{0.693}{t_{1/2}}, \quad (2.4)$$

For isotopes like uranium-238 (^{238}U), which decays through multiple pathways, the total decay constant is the sum of the constants corresponding to each mode. The half-life for each pathway is calculated using the reciprocal of its specific decay constant.

2.2.1 Alpha decay

This takes place when a nucleus that lacks stability ejects an alpha particle, shedding surplus energy in the process. The outcome is a new nucleus called the daughter nucleus with its mass number lowered by four and its atomic number decreased by two. Alpha particles carry a +2 charge and have a mass of four units as seen in Equation (2.5)

$$^{A}_{Z}X \longrightarrow {}^{A-4}_{Z-2}Y + {}^{4}_{2}He, \quad (2.5)$$

Here A is the number of nucleons, z is the proton number, Y is the parent nucleus, and Y is the daughter nucleus (Kanda et al., 2022).

2.2.2 Beta Decay

This involves three distinct mechanisms: the release of electrons, the emission of positrons, and the absorption of electrons by the nucleus. These transformations alter the nuclear charge by one unit without changing the mass number (Kanda et al., 2022). Beta particles are typically emitted at speeds approximated to the speed of light.

In negative beta decay (β^-), a neutron converts into a proton, releasing an electron and an antineutrino as seen in Equation (2.6).

$$^{A}_{Z}X \rightarrow \, ^{A}_{Z+1}Y + \beta^- + \bar{v}_e, \qquad (2.6)$$

Where A is the nucleon number, z is the proton number, Y is the parent nucleus, and Y is the daughter nucleus (Kanda et al., 2022).

2.2.3 Gamma Decay

This involves the emission of excess energy from an excited nucleus in the form of a gamma ray—a high-energy photon devoid of mass and charge. This process generally follows alpha or beta decay and facilitates the nucleus's transition to a stable state, as illustrated in Equation (2.7).

$$^{A}_{Z}X \rightarrow \, ^{A}_{Z}Y + \gamma, \qquad (2.7)$$

2.3 Environment Radiation

Radiation exposure in the environment arises from both natural and artificial sources (IAEA, 2004). Artificial radiation comes from isotopes like Iodine-131, Cobalt-60, Caesium-137, Sodium-22, and Manganese-54, which are produced in reactors or accelerators. These can significantly elevate radiation levels when released into the environment (Kanda et al., 2022).

Despite their risks, radioisotopes have diverse applications in medicine (pacemakers, imaging), safety devices (smoke detectors), industry (radiography), and energy production. However, areas near artificial radiation sources may be unsuitable for habitation due to increased concentrations of radioactive substances that occur naturally in the environment. To ensure safety, building materials should be evaluated for radioactivity, and exposure should be maintained at the lowest level reasonably achievable. Given that individuals spend more than 80% of their time within enclosed environments, evaluating indoor exposure to naturally occurring radioactive materials (NORM) is critically important..

Natural radiation includes cosmic rays and terrestrial radionuclides like uranium, thorium, and potassium-40 (Obid et al., 2011). These are found in soil, water, and even the human body. Radionuclides can still be detected today only if their half-lives are on the same scale as the age of the Earth.

There are four natural decay series: Uranium-235 (^{235}U); Uranium-238 (^{238}U); Thorium-232 (^{232}Th), and Neptunium-237 as shown in Table 2.1. However, Neptunium (^{237}Np) has decayed away due to its relatively short half-life (2.14 million years), leaving only uranium and thorium series active today.

Table 2.1: Natural decay series and half-lives (Obid et al., 2011).

Elements	First isotopes	Half-life	Last isotope
Uranium	^{238}U	4.5×10^{9}	^{206}Pb
Uranium	^{235}U	7.1×10^{8}	^{206}Pb
Thorium	^{232}Th	1.39×10^{10}	^{206}Pb
Neptunium	^{237}Np	2.14×10^{6}	^{209}Bi

Rocks and soils contain trace amounts of ^{238}U, ^{232}Th, and ^{235}U, undergo transformation into radon isotopes such as ^{222}Rn, ^{220}Rn, and ^{219}Rn, possessing half-lives of 3.82 days, 56, and 4 seconds, respectively (Tezcan et al., 2023). Due to its longer half-life, ^{222}Rn produced from the uranium-238 decay chain is the most significant contributor to indoor radon levels. This process is illustrated in Figure 2.1 (Obid et al., 2011).

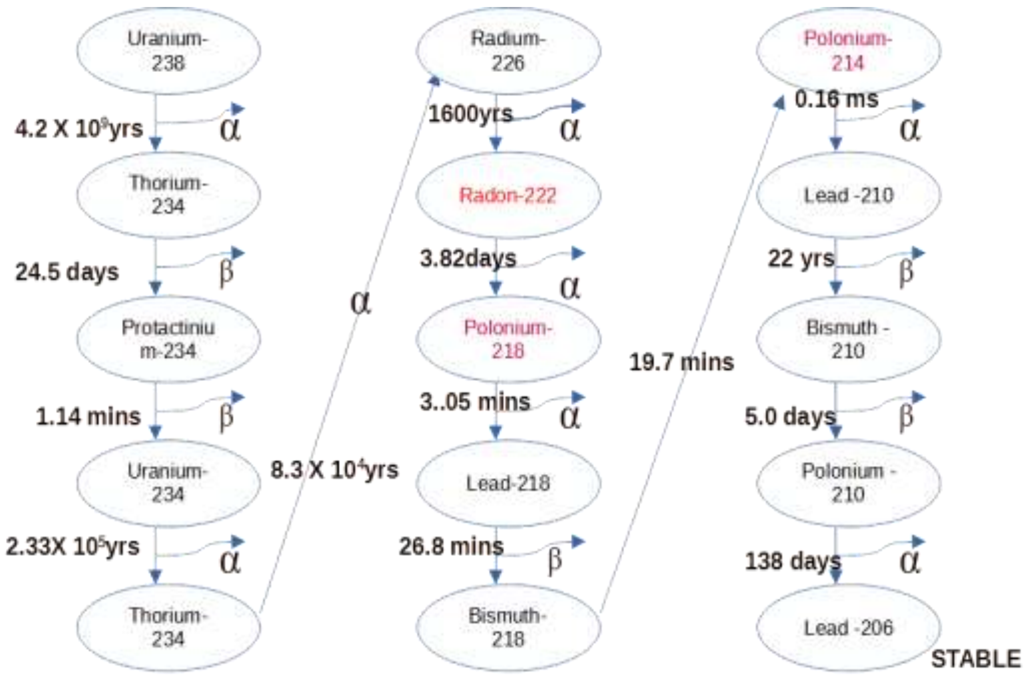

Figure 2.1: Uranium decay chain (Obid et al., 2011).

2.3.1 Ionising radiation

These radiations refer to energy that is powerful enough to disrupt the forces holding electrons within atoms, resulting in their release. When an atom or molecule absorbs sufficient energy to overcome the attraction between its nucleus and electrons, the electrons are expelled. This form of radiation is typically invisible, consisting of waves or particles that are not easily detected. Figure 2.2 displays ionising radiation across a spectrum of frequencies and wavelengths, illustrating how ionisation rates vary depending on wavelength.

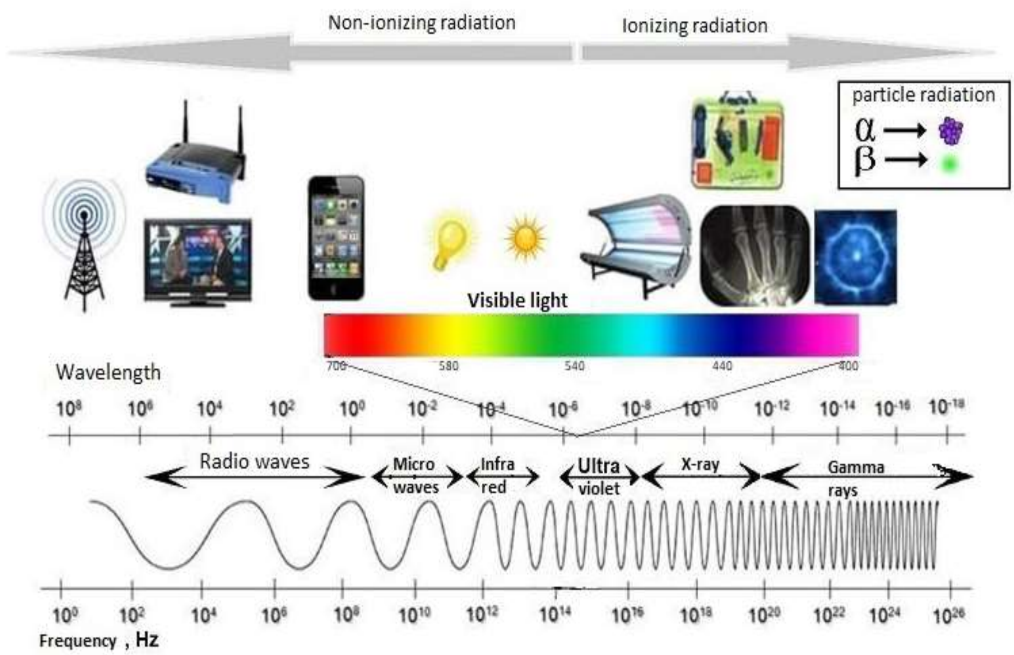

Figure 2.2: Spectrum of ionising radiation by wavelengths (Yousif et al., 2022).

Gamma and X-rays are types of electromagnetic radiation that feature very low wavelengths and very high frequencies. Their elevated energy levels enable them to penetrate materials and make them the only types capable of causing ionisation (Yousif et al., 2022).

2.3.2 Non-ionising radiations

These are low-energy form that lack the capacity to remove electrons from atoms or molecules. They include visible light, infrared, ultraviolet, microwave, and radio-frequency emissions, such as those from mobile phones. Generally, these types of radiation pose minimal risk to human health.

2.4 Radon in rocks and soil

All rocks contain some amount of uranium, though most have only small concentrations typically between one to three parts per million (ppm). This implies that 500 tons of rock would contain roughly 0.5 to 1.5 kilograms of uranium

(Elsesmita et al., 2022). Soil forms through the physical and chemical weathering of rocks, so it commonly inherits trace uranium levels from its parent material. Certain rock types, such as black shales, light-colored volcanic rocks, and granites, tend to have elevated uranium content (Elsesmita et al., 2022).

The surrounding soils and rocks can hold uranium concentrations as high as 100 parts per million (ppm). The variation in uranium levels across different regions of Uganda contributes to differences in indoor ^{222}Rn levels in dwellings and workplaces. Interestingly, some buildings in high-uranium areas show low radon levels, while others in low-uranium zones exhibit elevated radon concentrations (Kazwini et al., 2020). This suggests that radon levels are influenced not only by geology but also by factors such as construction materials, building age, and ventilation systems

2.5 Radon mitgration

While uranium and radium remain fixed within solid rock and soil, radon is a gas and can move more freely. It escapes through fractures and pores in rocks and soil, entering the surrounding environment (Appleton et al., 2020). The level of radon entering a structure is influenced by how readily it can move through available gaps and pathways. If radon can move efficiently through pore spaces and cracks before decaying, it is more likely to accumulate indoors.

Radon’s movement through soil is affected by moisture content, porosity (the proportion of pore space), and how well these pores are connected factors that determine porosity, as illustrated in Figure 2.3.

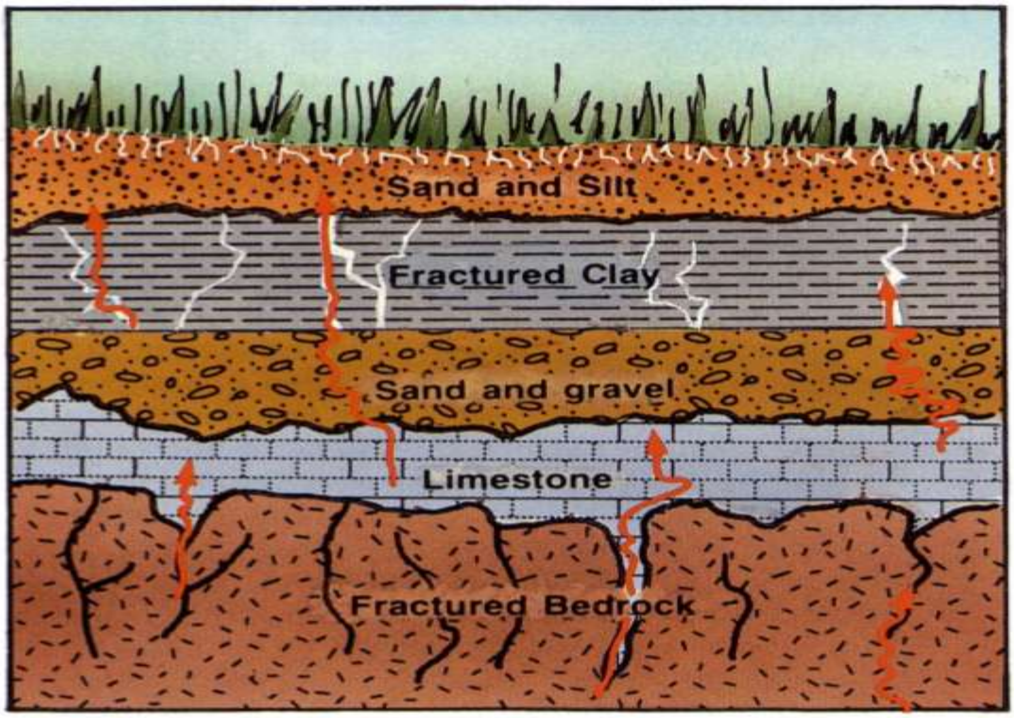

Figure 2.3: Pathways of radon migration through soil environment (Appleton et al., 2020).

Porous soils such as sand and gravel allow radon to travel more readily than dense soils such as clay. Cracked rocks and soils also facilitate faster radon movement (Appleton et al., 2020). In water-saturated environments, radon disperses more slowly than in air. It can travel up to 6 feet in wet soil before decaying, but only about 1 inch in dry soil. This is because water slows the movement of radon gas, whereas air allows it to move more quickly through pores and fractures.

Dry, permeable soils and bedrock such as those found on hillsides, in glacial deposits, or fractured rock formations are more likely to exhibit high radon concentrations. These areas permit radon-laden air to travel farther before decaying, even when the ^{222} Rn levels in soil air is within the typical range of 200 to 2,000 Bq/m^3 (Appleton et al., 2007).

2.5.1 Radon entry into buildings

Radon infiltrates buildings through multiple routes, including cracks in foundations and pores in surface-level soil (Elsesmita et al., 2022). The rate at which ^{222}Rn enters a structure is influenced due to variations in air pressure within the ground and the building and the ease with which ^{222}Rn enters a building is also affected by the permeability of the soil surrounding the foundation. Air originating from disrupted areas or gravel layers can infiltrate indoor spaces through cracks and flaws in the structure as well as the porosity of the soil adjacent to the basement facilitates the movement of air from disturbed zones and gravel beds into buildings through structural defects

Variations in temperature and atmospheric pressure between the interior and exterior of a building can cause ^{222}Rn to enter through gaps in concrete floors, wall cracks, utility line fittings, and even opening the doors and windows, as depicted in Figure 2.4.

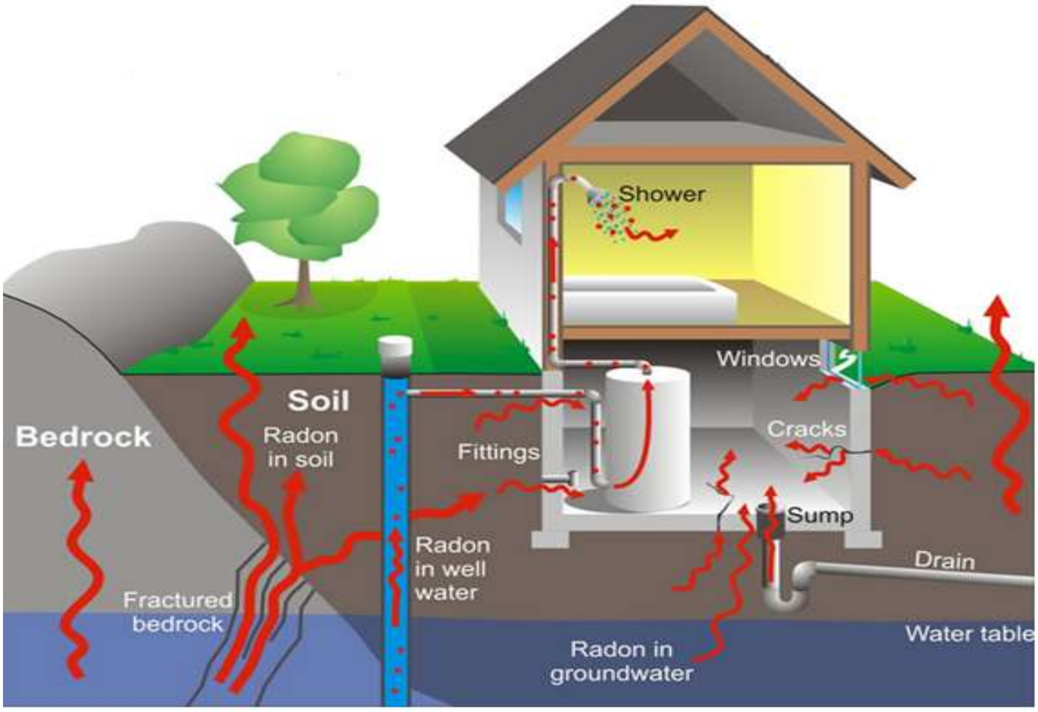

Figure 2.4: Pathways for ^{222}Rn infiltration into indoor air (Elsesmita et al., 2022).

Research has demonstrated that ^{222}Rn concentrations are typically higher in basements and ground floors compared to upper levels (Elsesmita et al., 2022). Additionally, groundwater pumped into buildings especially for showers can introduce radon, as its density allows it to dissolve into subsurface water.

During basement construction, specific steps are taken to reduce radon entry. These include excavating a pit, laying footings, and placing coarse gravel beneath the slab. After the basement walls are constructed, they are carefully sealed to eliminate any openings between the structure and the adjacent soil—commonly designated as the disturbed zone. This area, typically composed of foundation debris such as cement and rocks, can serve as a source of radon emission factors such as soil type and permeability within the disturbed zone, the composition under the gravel bed, the uranium content of local rock, and soil moisture levels all influence radon concentrations in specific areas.

A report published by the United Nations Environment Programme in 2016 indicates that typical indoor radon levels average approximately 100 Bq/m^3. However, levels can vary widely from as low as 1 Bq/m^3 to as high as 500 Bq/m^3 (Matovu et al., 2021). Poor ventilation in enclosed spaces like buildings, caves, or mines often leads to higher radon accumulation compared to outdoor environments.

2.6 Radon dose rates

Radon dose rates refer to the level of radiation an individual is exposed to over a given time due to the availability of ^{222}Rn gas. The amount of radioactive substances in the lungs is affected by the interaction between radon decay products and the body's clearance mechanisms (Farkas et al., 2020). Such concentrations are commonly quantified using units like picocuries per liter (pCi/L) or becquerels per cubic meter (Bq/m^3), which indicate the frequency of radioactive decay within a specific air volume.

Radon and its daughter particles are recognised as the dominant contributors to naturally occurring background radiation and are strongly linked to increased lung cancer risk (Shahbazi et al., 2013). The harmful alpha particles given off by radon's decay products, which can accumulate in lung tissue, are quantified in millisieverts (mSv).

To express radon dose rates as effective doses, a conversion factor is applied based on the type of radiation emitted and the standard tissue weighting factors used in human dosimetry (Papenfuß et al., 2022).Assuming equilibrium between radon and its daughter partcles in the air, the commonly accepted conversion is 1 pCi/L = 37 Bq/m³. The annual effective dose, measured in millisieverts, is determined by applying a dose conversion factor—typically ranging from 9 to 10 mSv per 1000 Bq/m³—to the measured ^{222} Rn levels in becquerels per cubic meter.

Radon exposure limits vary across countries (Riudavets et al., 2022). WHO recommends a reference level of 100 Bq/m³ (equivalent to 2.7 pCi/L) as the threshold for initiating mitigation efforts (Vimercati et al., 2018). If radon levels exceed this benchmark, preventive and corrective measures should be implemented to reduce exposure.

2.7 Health risks from radon exposure

Inhalation is the primary pathway where the individuals are exposed to ^{222} Rn and its radioactive decay products (Maier et al., 2021). The health risks are mainly attributed to decay products with short half-lives like polonium-218 and polonium-214, which emit alpha particles that are particularly damaging to human tissue (Lorenzo et al., 2019). The harmful effects of ^{222} Rn stem from its radioactive decay, which can damage cells and tissues, ultimately leading to lung cancer. Notably, radon exposure does not show immediate symptoms, making it difficult to detect without testing.

Because inhaled air reaches the lungs directly, radon and its daughter particles primarily affect the respiratory system (Lorenzo et al., 2019), as observed in Figure 2.5.

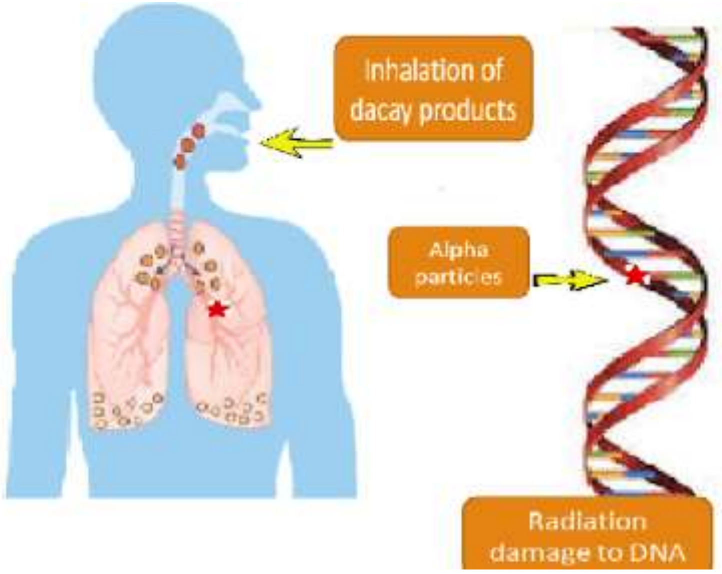

Figure 2.5: Pathway of ^{222}Rn and its decay products into the lungs (Appleton et al., 2020).

Once inhaled, radon atoms undergo further radioactive disintergration within the lungs, releasing radiation that can bind to lung tissues and potentially cause DNA mutations (Appleton et al., 2020). Larger particles tend to settle in the upper airways and are expelled by the body's mucociliary system, whereas finer particles are capable of reaching the deeper parts of the respiratory tract. The accumulation of radon progeny within the respiratory tract depends on the size of the inhaled particles.

Smokers face an increased likelihood of developing lung cancer due to ^{222}Rn exposure compared to non-smokers. According to WHO, ^{222}Rn is the second most common cause of lung cancer after tobacco use (Grzywa et al., 2020). ^{222}Rn is classified as a human carcinogen based on studies involving animals, cell cultures, and epidemiological research in both the general population and mining communities (Riudavets et al., 2022). Evidence from these studies confirms the connection between ^{222}Rn exposure and cancer development. Numerous case-control studies have assessed radiation exposure in residential and occupational settings (Darby et al., 2004), aiming to support the establishment of radon monitoring programs and improve measurement techniques in buildings under construction.

Research has consistently shown that miners working underground are at greater risk of getting lung cancer due to a prolonged ^{222}Rn exposure and its daughter products (Lorenzo et al., 2019). However, recent case-control studies have sparked debate by suggesting a lower incidence of lung cancer among individuals exposed to ^{222}Rn levels ranging from 50 Bq/m³ to 123 Bq/m³, in comparison to those exposed to levels below 25 Bq/m³ (Maier et al., 2021).

2.8 Comparision of indoor radon regulations and health impacts

Various regulatory bodies have established different standards for acceptable radon exposure levels (Belete et al., 2021). The Miner's Safety and Health Act (MSHA) is designed to protect underground miners, while the Occupational Safety and Health Act (OSHA) regulates radon exposure for non-mining workers. MSHA advises that ^{222}Rn levels in occupational settings should not go beyond 100 Bq/m³.

Both Environmental Protection Agency (EPA) and WHO recommend action levels for radon exposure to range between 100 and 300 Bq/m³ (Vimercati et al., 2018). If indoor radon levels surpass these thresholds, building owners are required to implement mitigation strategies. Research has shown that countries have adopted varying limits for indoor radon to reduce lung cancer risks (Appleton et al., 2020; Elsesmita et al., 2022; Riudavets et al., 2022). Despite its health implications, occupational exposure to radon-222 has been largely overlooked and warrants consideration alongside residential settings in public health assessments

Table 2.2: Recommended indoor ^{222}Rn concentration levels (Catão et al., 2022; Lorenzo et al., 2019).

Country	Occupation building (Bq/m^3)	Dwelling (Bq/m^3)
Austria	300	300
Canada	300	200
China	200	300
France	100	300
Georgia	300	200
Italy	100	200
Portugal	300	300
Republic of Moldova	300	150
Spain	150	200
Switzerland	300	300
United Kingdom (UK)	300	200
United States of America	300	148

2.9 Radon detection methods

Although ^{222}Rn decay products like ^{218}Po and ^{214}Po contribute most exposure from ^{222}Rn (Kendall et al., 2002), ^{222}Rn gas concentration is commonly used as a reliable indicator due to its ease of measurement and cost-effectiveness.

Radon levels can be assessed using both short and long-term testing techniques (Pantelić et al., 2019; Tsapalov et al., 2021). Long-term radon monitoring is commonly conducted using passive detection devices, including electret ion chambers and alpha-track detectors, while activated charcoal detectors are suitable for short-term assessments. For continuous and real-time tracking, active devices like Continuous Radon Monitors (CRMs) are preferred.

Table 2.3: Common of radon detection and their features (Pantelić et al., 2019)**.**

Detectors	**Active/ Passive**	**Sampling periods**	**Cost**
ATDs	Passive	1-12 months	Low
ACD	Passive	2-7days	Low
EICs	Passive	5 days-1 year	Medium
CRMs	Active	1 hour- year (s)	Medium
EIDs	Active	1 hour – year (s)	High

ATDs are commonly positioned for about a twelve month radon monitoring in buildings. Electret ion chambers (EICs) are more frequently used and can be configured for daily, weekly, or monthly measurements. Continuous Radon Monitors (CRMs) have emerged as the most widely utilized instruments for real-time radon measurement, offering automated, time-sensitive data that allows for precise calculation of integrated radon levels. CRMs are equipped with scintillation sensors to detect radon concentrations effectively.

CHAPTER THREE: MATERIALS AND METHODOLOGY

3.1 Overview

This chapter is structured into four key sections: the study area, radon activity concentration measurements, exposure dose assessment, Data processing and approaches used for data analysis and statistical analysis techniques.

3.2 Geological scope

The research aimed to quantify the ^{222}Rn and estimate the exposure levels among dwellers and workers in selected buildings within Kampala City Authority, Uganda. With a daily population estimated at 2.9 million—60% of whom are employed— Kampala is a highly populated metropolitan area, geographically positioned at 0° 20' 51.3456" North latitude and 32° 34' 57.0720" East longitude, spanning an area of approximately 84,519 km^2 (or 3,263.3 square miles). The study focused on five administrative divisions: Nakawa, Central, Makindye, Rubaga, and Kawempe, chosen for their geological features, particularly the presence of igneous and sedimentary rocks known to contain uranium, as illustrated in Figure 3.1.

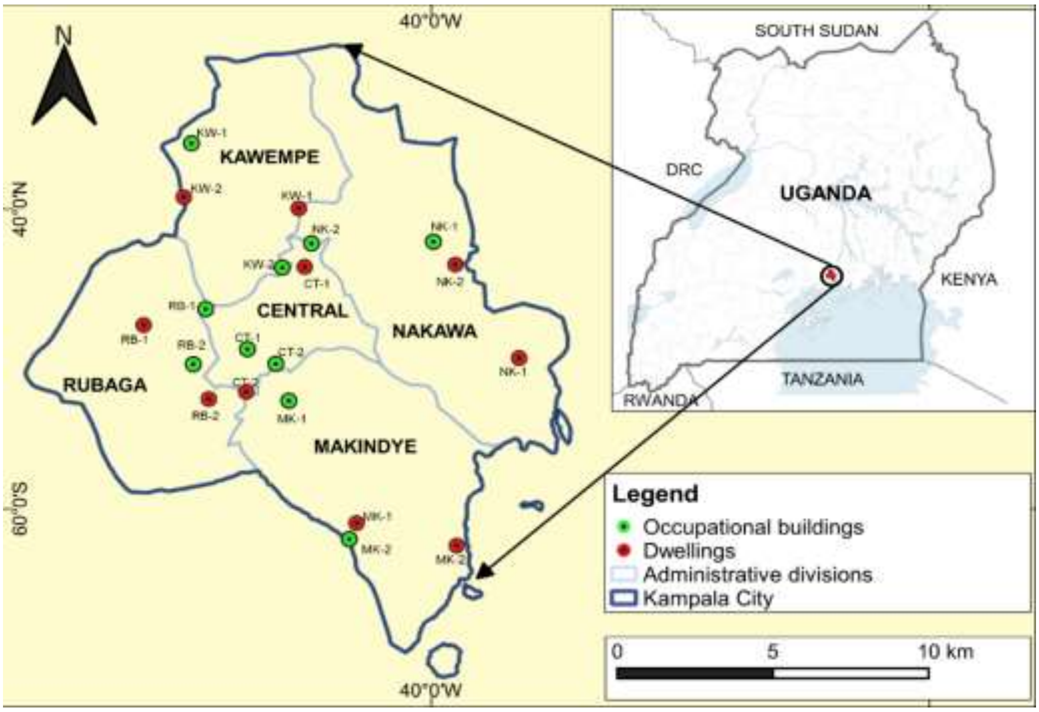

Figure 3.1: Map of Kampala Capital City Authority highlighting the study locations.

Kampala experiences a tropical savanna climate, with an average yearly ambient temperature of 22°C and yearly rainfall around 1,300 mm. The seasons alternate between wet and dry, with the heaviest rains falling in April and October. Rainy periods span March–May and September–November, while drier months occur from December–February and June–August.

Radon measurements were conducted in ten occupational buildings and ten dwellings selected randomly. In workplace settings, radon measurements were conducted across three distinct levels: basement, ground, and first floor in structures equipped with basements; and ground, first, and second floors in buildings lacking basement levels. For residential buildings, sampling was concentrated in rooms located at ground level. The altitudes of the surveyed locations varied from 1170 to 1259 meters above mean sea level

3.3 Radon activity concentration measurements

Indoor radon concentrations (^{222}Rn) were recorded using the Radon Sentinel Model 1030. Measurements were conducted from June to December 2023 across three floors within each workplace facility, as well as in the living and sleeping areas (bed rooms) of the chosen dwelling units. Comprehensive descriptions of the monitored rooms are available in Tables A1 and A2, located in Appendix A.

For reliable measurement results, the monitoring device was installed at a height of roughly 1.2 meters above the floor in workplace environments and about 0.8 meters in dwelling settings. To minimize the impact of airflow and nearby structural elements, the device was placed no closer than 0.5 meters from any walls, windows, or doors, as shown in Figure 3.2(a).

Figure 3.2: (a) Set-up of Radon Sentinel Monitor (model 1030), and (b) Radon sentinel Detector.

The device operated for 8 hours during day time between 9:00 am and 5:00 pm in workplaces, and between 9:00 pm and 5:00 am overnight in dwelling settings.

During operation, the device allowed air to pass through a thoron discriminator, enabling ^{222}Rn to enter due to its longer half-life. The ^{222}Rn then reached the scintillation chamber, where light pulses were generated and counted. These counts indicated the presence of ^{222}Rn decay products, specifically ^{218}Po and ^{214}Po which were detected using a photomultiplier tube (PMT). The PMT, powered by Electron High Voltage (EHT), amplified the signal and accelerated the electrons within the counting chamber.

Once detected, the counts were stored in a chip memory circuit and converted into ^{222}Rn concentration values (in Bq/m^3), a calibration coefficient supplied by Sun Nuclear Corporation was applied to ensure accurate measurement results (Pant et al., 2016).

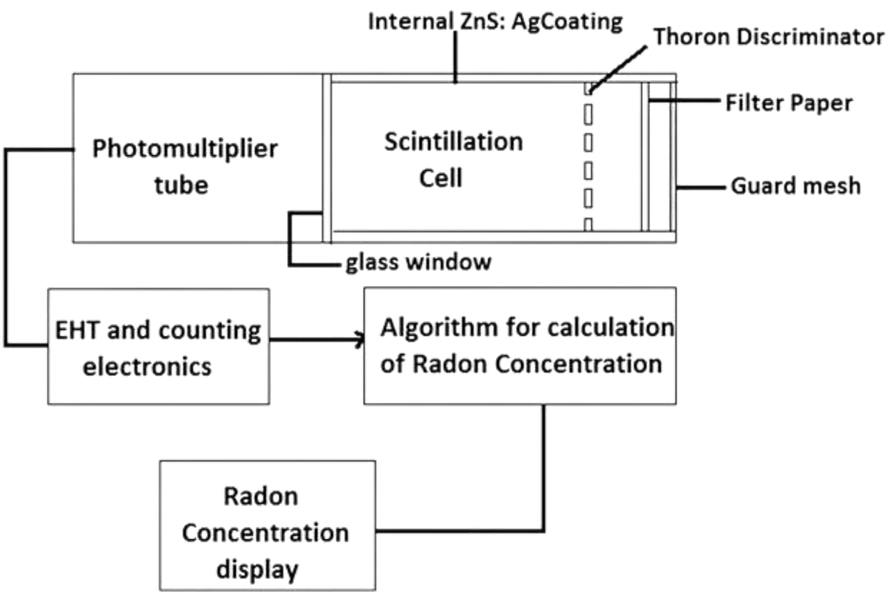

Figure 3. 3: Illustrative layout of a radon sentinel monitoring device (Teiri et al., 2021).

3.4 Dose estimation and risk assessment

3.4.1 Computation of annual effective dose (ED)

The ED resulting from exposure to radon gas (^{222}Rn) for both dwellers and workers was calculated using the dosimetric approach recommended by the United Nations Scientific Committee on the Effects of Atomic Radiation (UNSCEAR) (Cucoş et al., 2025; Tezcan, Aközcan et al., 2023). The formula used is presented in Equation (3.1):

$$\text{ED (mSv/ year)} = C_{Rn} \times H \times F_R \times D \times T, \qquad (3.1)$$

C_{Rn} represents the detected ^{222}Rn levels measured in Bq/m³, H being the occupancy factor, set at 0.5 (12 hours/day) for dwelling settings and 0.33 (8 hours/day) for workplaces, F_R is the equilibrium factor between ^{222}Rn and its daughter particles, estimated as 0.4, D is the dose conversion coefficient, taken as 9.0 nSv/h per Bq/m³ based on UNSCEAR guidelines and T denotes the total annual time of exposure, which is 8760 hours.

3.4.2 Estimating annual equivalent dose and lifetime cancer risk (LCC)

The annual lung equivalent dose (ERD) was calculated based on a specific using Equation (3.2), as outlined by Azhdarpoor et al. (2021):

$$\text{ERD (mSv/ year)} = \text{ED} \times W_R \times W_T, \qquad (3.2)$$

Here, W_R represents weighting factor to radiation exposure assigned to alpha particles, which is 20, while W_T denotes the tissue weighting factor for the lungs, set at 0.12.

The excess lifetime cancer risk (ELCR) from exposure of ^{222}Rn was assessed using Equation (3.3) as applied (Machraoui et al., 2024; Tezcan et al., 2023).

$$\text{ELCR} = \text{ED} \times T_{LE} \times F_{CR}, \quad (3.3)$$

Where; T_{LE} is the mean life expectancy, estimated at 70 year , and F_{CR} is the fatal cancer risk coefficient, valued at 5.5×10^{-2} Sv^{-1} based on the International Commission on Radiation Protection (ICRP, 2007).

3.4.3. Lung cancer incidence (LCC) estimation

The projected number of LCC per million individuals annually due to the level of ^{222}Rn exposure which was assessed using Equation (3.4) (Azhdarpoor et al., 2021; Lin et al., 2024).

$$\text{LCC} = 18\times10^{-6} \times \text{ELCR}, \quad (3.4)$$

Here, 18×10^{-6} mSv/year is the risk coefficient for lung cancer induction.

3.5. Data analysis and statistical methods

Radon-222 concentrations were recorded over 8-hour intervals in bothdwellings and occupational settings using a CRM. The results were expressed in form of arithmetic means accompanied by standard error (AM ± SE).

The dataset was analysed using OriginPro 2024b, a statistical and graphing software developed by OriginLab Corporation, USA.To explore the relationship between radon levels and indoor environmental variables including temperature and humidity, Pearson correlation analysis and hierarchical clustering techniques were employed.

CHAPTER FOUR: RESULTS AND DISCUSSION

4.1 Overview

This chapter outlines the results from indoor ^{222}Rn measurements conducted in selected occupational and dwellings buildings within Kampala City Authority. It presents average radon-222 (^{222}Rn) concentrations by building type, compares these values against both national and international safety benchmarks, and calculates the annual effective dose resulting from ^{222}Rn exposure. Additionally, it assesses the corresponding ELCR and estimates the number of radon-related LCC per million individuals annually.

4.2 Mean radon concentration levels in occupational buildings

Table 4.1 summarises the mean indoor ^{222}Rn levels, along with humidity and temperature readings, obtained from the selected occupational buildings. These values were derived from raw data presented in Appendix B. In basement areas, radon levels ranged from 17.5 ± 2.5 Bq/m³ to 95.8 ± 8.0 Bq/m³, averaging 46.3 ± 12.0 Bq/m³. Ground floor readings ranged between 8.7 ± 1.5 Bq/m³ and 79.2 ± 8.2 Bq/m³, averaging 35.1 ± 8.0 Bq/m³. On the first floor, ^{222}Rn levels spanned 9.4 ± 1.4 Bq/m³ to 74.3 ± 7.6 Bq/m³, with a mean of 22.8 ± 6.7 Bq/m³. Second-floor values ranged from 8.8 ± 1.4 Bq/m³ to 65.0 ± 6.2 Bq/m³, averaging 29.0 ± 13.1 Bq/m³.

All measured radon levels were below the ICRP's recommended action threshold of 200–300 Bq/m³ (Pantelić et al., 2019), indicating that occupational exposure remains within safe limits. Moreover, with the exception of poorly ventilated rooms within NK-1 were found to be less than the WHO- threshold of 100 Bq/m³ (Maier et al., 2021).

Table 4.1: Indoor ^{222}Rn concentration across various floors in occupational buildings.

N/S	Division	Site	Floor	Temp (°C)	Hum(%)	^{222}Rn (Bq/m³)
1	CENTRAL	CT-1	B	28.2	65	30.5 ± 2.9
			G	26.6	68	24.9 ± 2.8
			F1	28.0	60	18.4 ± 2.4
2		CT-2	B	26.9	54	19.4 ± 3.3
			G	28.4	48	8.7 ± 1.5
			F1	27.5	54	14.0 ± 2.7
3	NAKAWA	NK-1	B	29.3	54	38.6 ± 4.3
			G	28.3	53	28.4 ± 5.0
			F1	28.9	49	11.2 ± 1.3
4		NK-2	G	27.7	62	31.1 ± 3.9
			F1	26.4	61	15.2 ± 1.0
			F2	28.8	57	8.8 ± 1.4
5	MAKINDYE	MK-1	B	28.4	59	26.9 ± 3.8
			G	26.2	59	20.8 ± 2.3
			F1	26.4	60	15.6 ± 2.8
6		MK-2	B	26.1	72	95.8 ± 8.0
			G	25.2	69	61.4 ± 5.4
			F1	25.9	59	9.4 ± 1.4
7	RUBAGA	RB-1	G	28.6	61	15.9 ± 2.3
			F1	29.1	50	11.0 ± 1.9
			F2	28.4	62	9.9 ± 2.5
8		RB-2	G	28.5	63	79.2 ± 8.2
			F1	28.5	64	74.3 ± 7.6
			F2	27.8	65	65.0 ± 6.2
9	KAWEMPE	KW-1	B	28.7	53	17.5 ± 2.5
			G	29.8	53	11.4 ± 1.4
			F1	29.9	49	11.9 ± 2.3
10		KW-2	G	28.5	65	69.0 ± 4.1
			F1	28.5	63	47.1 ± 4.3
			F2	27.8	61	32.1 ± 8.0
STORAGE ROOMS WITH POOR VENTILATION						
11	NAKAWA	NK-1	G	26.7	60	194.8 ± 21.2
			F1	27.4	56	165.9 ± 14.6
			F2	28.1	59	136.7 ± 7.3

B; Basement; G: Ground floor; F1: First floor; F2: Second floor

Most of ^{222}Rn levels recorded were below the global average of 40 Bq/m³, except in specific areas such as the basement and ground floors of MK-2, all floors of RB-2, and the ground and first floors of KW-2 as seen in Table 4.1 and Figure 4.1).

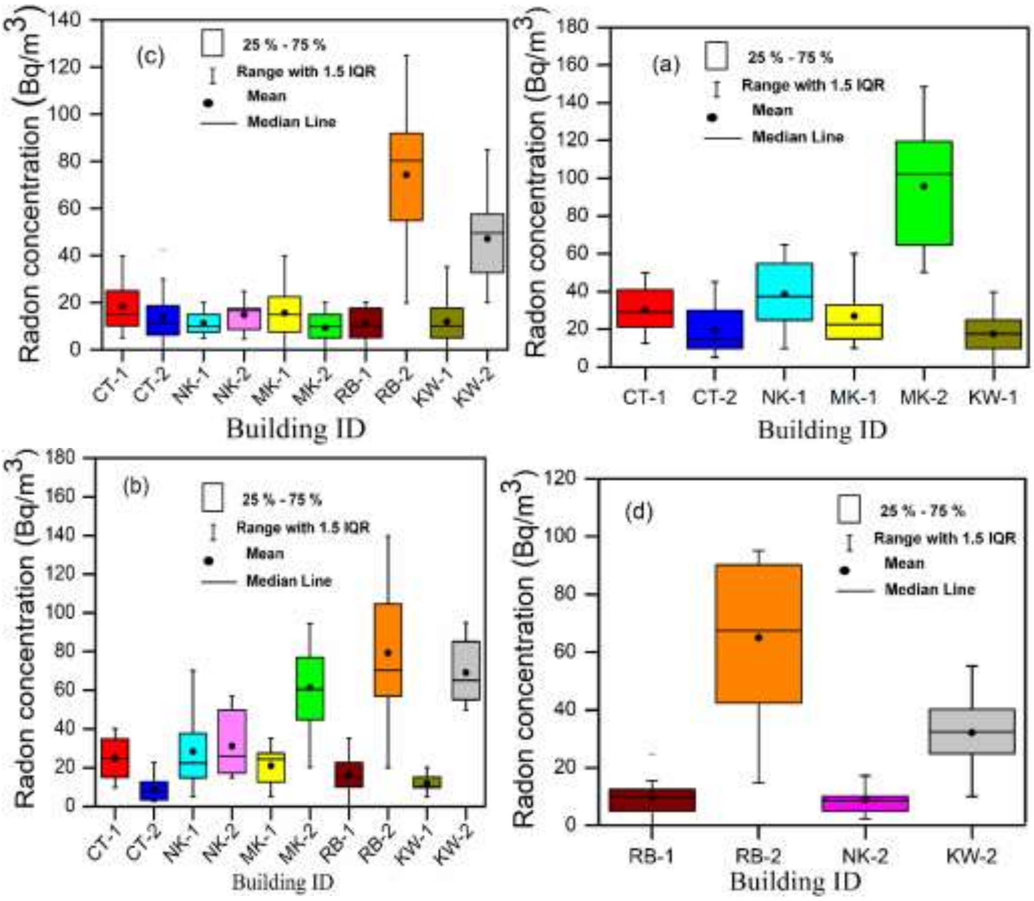

Figure 4.1: ^{222}Rn levels by floor: (a) basements, (b) ground floor, (c) first floor, and (d) second floor.

Radon concentrations varied notably across different floors, with the highest levels typically found in the basements, then ground, first, and second floors. This trend is largely due to radon infiltration from soil gas, which enters buildings through foundational cracks and utility openings. Numerous studies have confirmed elevated radon levels in lower floors due to their proximity to the ground (Cucoş et al., 2025; Teiri et al., 2021). Ventilation was a key factor—rooms with good airflow consistently showed lower radon levels, while poorly ventilated spaces had higher concentrations. No consistent relationship was found between radon levels and environmental factors like temperature or humidity, a finding also noted by Lin et al. (2024).

The highest radon level recorded was in the basement of MK-2, averaging 95.8 ± 8.0 Bq/m³. This outcome was linked to limited air circulation and the existence of coated wall that may trap radon gas. In contrast, the lowest readings were seen on the ground floor of CT-2 (8.7 ± 5.8 Bq/m³) and the second floor of NK-1 (8.8 ± 1.4 Bq/m³), likely due to mitigation strategies such as woollen carpets that reduce radon dispersion.

Among the buildings, RB-2 indicated the highest mean radon concentration at 79.2 ± 8.2 Bq/m³, followed by MK-2 at 55.5 ± 4.9 Bq/m³. These elevated levels were linked to poor ventilation and the age of the buildings which were notable, as RB-2 was constructed in the early 1990s and MK-2 following in the latter part of the same decade making them more susceptible to structural degradation and radon infiltration. Conversely, KW-2 and CT-2 showed the lowest mean radon concentrations, primarily due to the presence of well-functioning ventilation systems and generously sized windows, high-ceiling fans, and interior finishes like tiled floors and wooden wall coverings that reduce radon exhalation.

In poorly ventilated workspaces with structural damage (e.g., cracked walls and small windows), as presented in Figure 4.2, the ^{222}Rn levels on the ground floor ranged from 34.9 to 304.8 Bq/m³, while values on the first floor varied between 44.9 and 274.3 Bq/m³. On the second floor, concentrations were recorded between 97.2 and 189.2 Bq/m³ as indicated in Table B5 of Appendix B.

Figure 4.2: Structure cracks observed in measured workspaces.

In these poorly ventilated rooms, radon levels reached 194.8 ± 21.2 Bq/m³ on the ground level, 165 ± 14.6 Bq/m³ on the first floor, and 136.7 ± 7.9 Bq/m³ on the second floor—all exceeding the WHO's recommended threshold of 100 Bq/m³. (Cucoş et al., 2025), underscoring the impact of inadequate ventilation on radon accumulation.

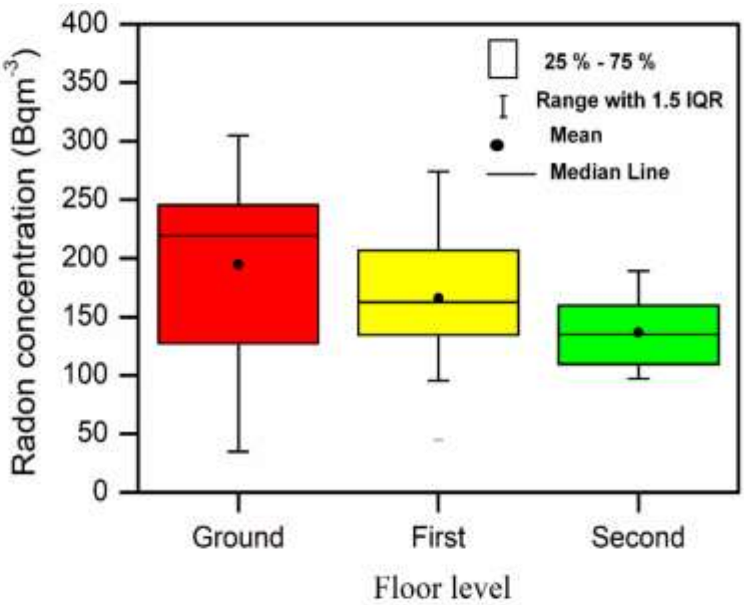

Figure 4.3: Average ^{222} Rn levels across levels in poorly ventilated workplaces.

4.3 Activity levels of ^{222}Rn concentration in dwellings

Table 4.2 presents the average ^{222} Rn levels, along with temperature and humidity data, for dwellings, based on raw data from Appendix C. Radon levels in bedrooms ranged from 25.6 to 271.3 Bq/m³, while sitting rooms showed concentrations between 20.3 and 59.8 Bq/m³. The overall average radon activity ranged between 15.3 ± 2.3 and 188.2 ± 8.2 Bq/m³, as illustrated in Figure 4.4 and detailed in Tables C1 and C2.

Table 4.2: Mean values of ^{222} Rn levels in selected dwellings.

N/S	DIVISION	Site	Temp (°C)	Humidity (%)	^{222}Rn (Bq/m³)
1	CENTRAL	CT-1	28	63	15.3 ± 2.3
2		CT-2	28.9	63	44.5 ± 17.5
3	NAKAWA	NK-1	27.9	62	188.2 ± 8.2
4		NK-2	27.4	64	105.5 ± 8.5
5	MAKINDYE	MK-1	27.5	59	135.9 ± 40.0
6		MK-2	28.3	62	59.3 ± 5.3
7	RUBAGA	RB-1	29.1	60	69.1 ± 17.1
8		RB-2	27.7	63	34.7 ± 6.7
9	KAWEMPE	KW-1	28.4	61	36.5 ± 10.6
10		KW-2	28.2	62	27.8 ± 7.8

The lowest recorded mean radon-222 (^{222}Rn) activity concentration was 15.3 ± 2.3 Bq/m³, observed at dwelling CT-1. This reduced level is primarily attributed to the building's efficient ventilation system, which includes louvred doors and windows, along with tiled flooring and wall surfaces that help limit radon accumulation.

Conversely, the highest average radon levels of 188.2 ± 8.2 Bq/m³ was measured at dwelling NK-1. The high readings are likely due to the availability of a concrete slab floor and the age of the structure, which dates back to the early 2000s. Over time, structural deterioration such as floor cracking may have created pathways for radon gas to infiltrate the indoor environment.

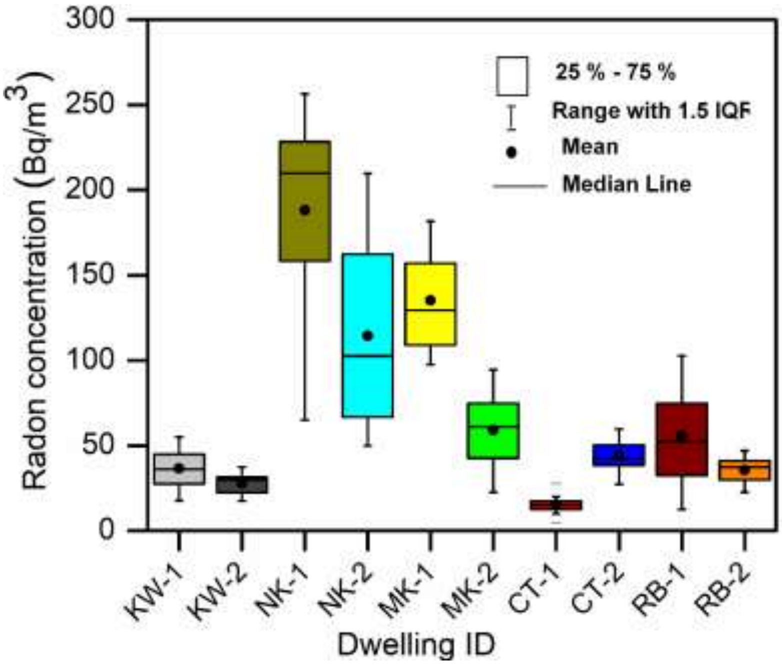

Figure 4.4: ^{222}Rn levels in bedrooms and sitting rooms of selected dwelling buildings.

As illustrated in Figure 4.4, several dwellings exhibited radon concentrations that surpassed the world wide average of 40 Bq/m³ (Tezcan et al., 2023). Particularly high levels were found in MK-1 in Makindye Division, and NK-1 and NK-2 in Nakawa Division, where ^{222}Rn levels were approximately two to five times above the global mean. These elevated values exceed the WHO's recommended limit of 100 Bq/m³, raising concerns about increased risks of radon-induced lung cancer.

Moderately elevated concentrations—about one to two times the global average—were observed in CT-2, MK-2, and RB-1. In contrast, other dwellings recorded radon levels below the global benchmark of 40 Bq/m³. These variations are likely influenced by a combination of factors, including local geology, limited ventilation, and building design features that may promote radon retention (Tezcan et al., 2023). The results highlight the importance of implementing site-specific mitigation measures and enhancing public education in regions exhibiting elevated radon concentrations.

4.4 Comparative analysis of indoor ^{222}Rn levels with other studies

Indoor radon concentrations in both occupational and residential buildings are shaped by a range of factors, including lifestyle patterns, geological conditions, and geographical location. Given the health effects of radon exposure, it is important to benchmark the readings of this study against data from other regions.

To facilitate this comparison, the radon-222 activity levels measured in Kampala's occupational and dwelling buildings were evaluated alongside results from similar studies conducted in other countries. These comparative values are summarised in Table 4.3.

Table 4.3: Comparative assessment of indoor ^{222}Rn levels across various workplaces and dwellings in relation to other studies

Study area	Localisation	Detection device	Radon (Bq/m³)	AM (Bq/m³)	References
Workplaces	Rawalpindi region and Islamabad Capital area – Pakistan	SSNTD – CR-39	12.0 to 293.0	62 ± 32	(Rahman et al., 2010)
Educational institutions	Romania	SSNTD – CR-39	28.0 to 729.0	211	(Cucoş et al., 2025)
Hospital Workplaces	Penghu and Kinmen – Taiwan	RADEX – MR107+	33.3 to 122.1		(Lin et al., 2024)
Workplaces	Tunisia	SSNTD – LR115	6.0 to 720.0		(Machraoui et al., 2024)
Campus buildings	Isfahan University of Medical Sciences – Iran	SARAD – RTM 1688	3.0 to 322.0		(Teiri et al., 2021)
Workplaces	Khartoum town – Sudan	SSNTD – CR-39	16.0 to 103.0	54 ± 9	(Elzain et al., 2023)
Workplace buildings	Rio de Janeiro City – Brazil	SSRD – RAD7	0.0 to 101.0	25.4	(Silva et al ., 2020)
Occupational buildings	Kampala Capital City Authority – Uganda	CRM –Sentinel 1030	8.7 to 95.8	30.8 ± 4.5	This study
Dwellings	Beijing City – China	SSNTD – CR-39	12.1 to 119.1	42.0 ± 13.7	(Wang et al. 2022)

Dwellings	Ebolowa town, Southern Cameroon	RADTRACK2 – CR-39	23.0 to 2620.0	135.6	(Mbida et al., 2023)
Residential buildings	Mazandaran Province, Iran	Polycarbonate track detector	53.1 to 218.9	124.5	(Cevik et al., 2010)
Dwelling	Jordan City – Jordan	SSNTD – CR-39	20.0 to 386.0		(Kazwini et al., 2020)
Residential dwellings	Southwest and South Greenland	SSNTD – CR-39	0.0 to 1291.0		(Hansen et al., 2023)
Dwelling	Edirne –Türkiye	Alpha GUARD-PQ 2000 PRO	12.0 to 82.0	31.1 ± 4.3	(Tezcan et al., 2023)
Residents	Southwestern – Nigeria	SSNTD – CR-39	12.0 to 445.0	69.1 ± 45.8	(Hansen et al., 2023)
Dwellings	Kampala Capital City Authority – Uganda	CRM –Sentinel 1030	15.3 to 188.2	71.6 ± 17.5	This study

This investigation compared indoor ^{222}Rn levels recorded in Kampala's occupational buildings and dwellings with data from similar environments in other countries, as outlined in Table 4.3. It is vital to note that variability in measurement techniques, equipment sensitivity, sampling protocols, and duration of monitoring can affect the comparability of findings across different studies.

Despite these methodological differences, the ^{222}Rn levels seen in occupational settings in Kampala were typically below the values documented in previous studies internationally, with the exception of Brazil, where comparable concentrations have been documented (Grzywa et al., 2020). In dwellings, the ^{222}Rn levels were also lower than those found in countries such as Cameroon, Iran, Greenland, and Jordan (Kazwini et al., 2020; Cevik et al., 2010; Hansen et al., 2023; Mbida Mbembe et al., 2023).

These global disparities in indoor radon levels are largely attributed to a number of geological and structural factors (Kellenbenz et al., 2021). Geological influences include differences in soil composition, natural uranium content, and environmental conditions such as humidity, which affect radon production and movement. Building-related factors such as construction materials, flooring types, ventilation systems, and architectural design (e.g., single-storey versus multi-storey structures), also significantly impact indoor radon accumulation. Together, these variables explain the broad range of radon concentrations reported worldwide.

4.5 Exposure dose estimation

4.5.1 Annual effective radiation dose for workers

The ED from inhaling ^{222}Rn by workers was determined by using Equation (3.1), based on the average ^{222} Rn levels measured across various floors and rooms in selected buildings, as illustrated in Figure 4.5. The corresponding annual ERD was derived using Equation (3.2), with results presented in Table D1 of Appendix D.

The annual ED values varied between 0.09 ± 0.02 and 1.00 ± 0.08 mSv/year. The maximum dose was detected in the basement of MK-2 situated in Makindye Division, whereas the minimum readings were found on the ground floor of CT-2 in central division and the first floor of MK-2. Floor-based averages showed 0.40 ± 0.13 mSv/year in the basement, 0.37 ± 0.08 mSv/year on the ground level, 0.24 ± 0.07 mSv/year on the first floor, and 0.30 ± 0.14 mSv/year on the second floor.

These values fall within the occupational exposure thresholds set by the WHO and ICRP (1 mSv/year) (Silva and Silva-Filho, 2020; Elzain, 2023; Rahman et al., 2010). Nevertheless, in high-risk areas like the inadequately ventilated storage facilities at NK-1, ED values exceeded the safety threshold, with the annual ED reaching 2.03 ± 0.22 mSv/year on the ground floor, 1.73 ± 0.15 mSv/year on the first floor, and 1.42 ± 0.08 mSv/year on the second floor.

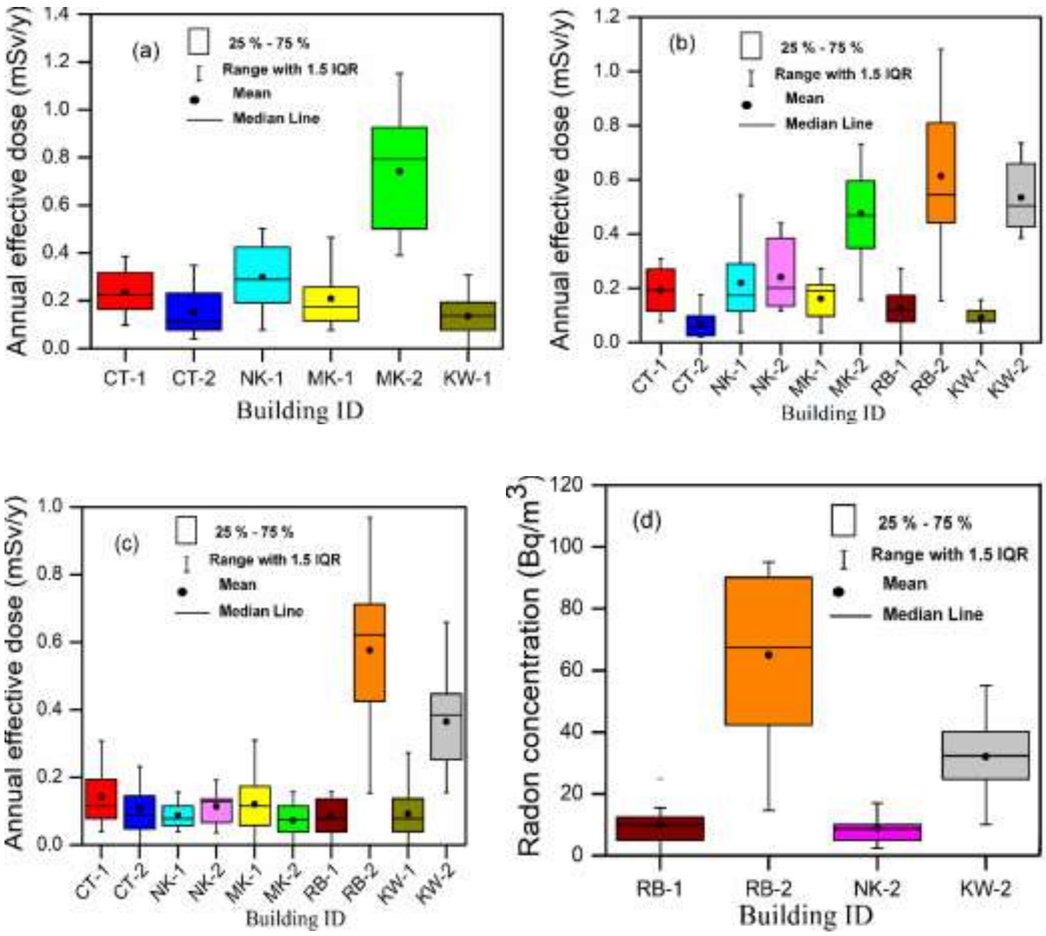

Figure 4.5: Annual ED dose exposure for workers at different levels in different buildings.

The ERD to the lungs ranged from 0.22 ± 0.02 to 2.40 ± 0.19 mSv/year. Average ERD values by floor were 0.95 ± 0.30 mSv/year in the basement, 0.88 ± 0.20 mSv/year on the ground floor, 0.57 ± 0.17 mSv/year on the first floor and 0.72 ± 0.33 mSv/year on the second floor.

These differences reflect the influence of proximity to ^{222}Rn sources (e.g., soil and foundations) and ventilation efficiency, with lower floors generally experiencing higher radon infiltration and reduced air exchange.

4.5.2 Annual effective radiation dose for Dwellers

The annual ED associated with respiratory exposure of ^{222}Rn by dwellers was determined using Equation (3.1), which was based on the mean ^{222}Rn concentrations measured in the selected dwellings, as illustrated in Figure 4.6. The ERD to the lungs was further derived through Equation (3.2), with the corresponding results presented in Table D2 of Appendix D.

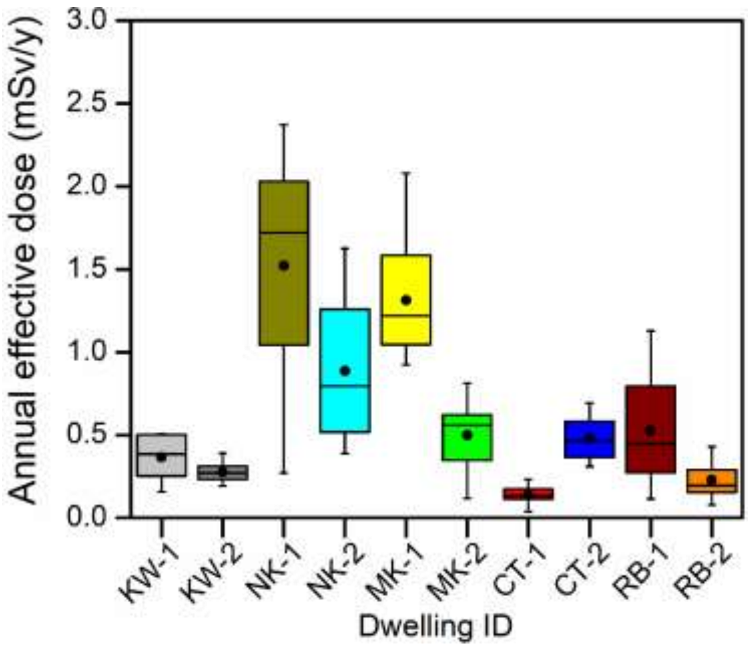

Figure 4.6: Annual ED for dwellers across different dwellings.

The equivalent dose (ED) varied between 0.16 ± 0.02 and 1.96 ± 0.09 mSv/year, with a mean of 0.75 ± 0.18 mSv/year. This mean value falls below the global environmental exposure reference level of 1.15 mSv/year reported by Azhdarpoor et al. (2021). However, some dwellings particularly NK-1 and MK-1—recorded higher doses of 1.96 ± 0.09 and 1.41 ± 0.42 mSv/year, respectively. While these elevated readings suggest limited concerns, the entire exposure levels across the study area were notably below the values reported in previous research, including the 2.6 mSv/year noted by Dadashpoor et al. (2025).

4.6 Excess lifetime cancer risk (ELCR) and lung cancer cases per million persons per year

ELCR and the projected LCC per million individuals annually were determined using Equations (3.2) and (3.3), respectively. Results for both occupational and dwelling environments are presented in Tables D1 and D2 of Appendix D.

The results for different working environments are contained in Appendix D, specifically Tables D1 and D2. In basement sections, ELCR values ranged from 6.93 ± 1.16 to 38.5 ± 3.08, with a mean of 11.79 ± 4.81, corresponding to about 7.14 ± 2.25 LCC per million persons annually. On ground floors, ELCR values varied from 3.47 ± 0.77 to 31.57 ± 3.47, with an average of 14.09 ± 3.20 mSv/year, equivalent to 6.59 ± 1.49 LCC. Among first-floor occupants, ELCR ranged from 3.85 ± 1.16 to 29.65 ± 2.67, averaging 9.13 ± 2.67, which translates to 4.27 ± 1.25 LCC per year. On second floors, values spanned 3.47 ± 0.77 to 26.18 ± 2.31, with a mean of 11.55 ± 5.32, corresponding to approximately 5.40 ± 2.49 LCC annually.

The highest recorded ELCR, measured at 38.50 ± 3.08, was found in the basement area of building MK-2, corresponding to an estimated 18.00 ± 1.44 LCC per million individuals each year. In contrast, the minimum risk of 3.47 ± 0.77 was recorded on the ground floor of CT-2, equivalent to about 1.62 ± 0.36 LCC annually.

Exceptionally high ELCR values were observed in poorly ventilated storage rooms at NK-1, with readings of 78.16 ± 8.47, 66.61 ± 5.78, and 54.67 ± 3.08 on the ground, first, and second floors, respectively. These corresponded to 36.54 ± 3.96, 31.14 ± 2.70, and 25.56 ± 1.44 LCC per million people per year—well above internationally accepted averages (Mbida et al., 2023).

These findings clearly demonstrate that adequate ventilation is a decisive factor in mitigating indoor radon exposure and lowering the associated risk of lung cancer in occupational environments.

In dwelling settings, The ELCR values varied between $(6.16 \pm 0.77) \times 10^{-4}$ and $(75.46 \pm 3.47) \times 10^{-4}$, with a mean of $(28.72 \pm 7.00) \times 10^{-4}$. This corresponds to an estimated 13.43 ± 3.27 LCC per million persons each year.

CHAPTER FIVE: CONCLUSIONS AND RECOMMENDATIONS

5.0 Overview

This section outlines the final key aspects drawn from the findings discussed in Chapter Four and outlines key recommendations based on the study's outcomes.

5.1 Conclusion

Indoor concentrations of ^{222}Rn were measured in ten workplace facilities and in ten dwelling units within Kampala Capital City Authority using a continuous measurement device (Radon Sentinel, Model 1030). In all surveyed locations, the detected radon levels were consistently below the WHO's recommended limit of 100 Bq/m^3.

The highest ^{222} Rn levels were detected in basement areas, averaging 46.3 ± 12.0 Bq/m^3. Radon levels generally declined with increasing floor height, although an unexpected rise was noted on second floors, where the average was 29.0 ± 13.1 Bq/m^3 higher than the 22.8 ± 6.7 Bq/m^3 recorded on first floors.

Structures with inadequate ventilation, such as RB-2 and MK-2, exhibited increased concentrations of ^{222} Rn, whereas well-ventilated structures like CT-2, RB-1, and KW-1 showed significantly lower concentrations. In dwellings, the mean ^{222} Rn levels was 71.6 ± 17.5 Bq/m^3. The maximum level, 180.0 ± 11.5 Bq/m^3, was observed in dwelling NK-1 located in Nakawa Division, most likely resulting from structural defects such as cracks in the concrete floor.

The annual ED estimates for both workers and dwellers were calculated and found to be within the acceptable limit of 1 mSv/year, as recommended by WHO and

ICRP. However, approximately 30% of the dwellings exceeded this limit, indicating the need for targeted mitigation efforts.

5.2 Recommendation

Although radon concentrations in all occupational buildings were within safe limits, nearly one-third of the surveyed dwellings surpassed the WHO guideline of 100 Bq/m^3. While occupational exposure doses remained below the 1 mSv/year benchmark, some dwellings recorded doses varied between 1.10 and 1.52 mSv/year, exceeding the recommended threshold. Based on these findings, the following recommendations are proposed.

i. Implement urgent remedial measures in high ^{222}Rn dwellings by improving ventilation and closing up cracks in floors and walls to reduce ^{222}Rn infiltration.

ii. Promote public education and awareness through outreach campaigns that inform residents about radon hazards, encourage routine testing, and share practical mitigation techniques suitable for homeowners.

iii. Strengthen regulatory frameworks and building policies by mandating radon-resistant construction practices in new developments and launching government-supported initiatives for testing and remediation in existing dwellings.

iv. Support continuous monitoring and research, including periodic surveys to track ^{222}Rn levels across Kampala. The data gathered should act as a foundation for future studies and help evaluate the success of implemented mitigation measures.

v. Develop predictive modelling tools to estimate` radon distribution across different building types and geographical zones. These models should account for variables such as construction materials, ventilation system capacity, room dimensions, and regional geological characteristics.

REFERENCES

Al-Kazwini, Akeel T., Mohannad M. Al-Arnaout, and Tiba R. Abdulkareem. 2020. “Radon-222 Exposure and Dose Concentration Levels in Jordanian Dwellings.” *Journal of Environmental and Public Health* 2020. doi:10.1155/2020/6668488.

Appleton, J. D. 2007. “Radon: Sources, Health Risks, and Hazard Mapping.” *Ambio* 36(1): **85–89**. doi:10.1579/0044-7447(2007)36.

Appleton, J. D., D. G. Jones, J. C. H. Miles, and C. Scivyer. 2020. “Chapter 18 Radon Gas Hazard.” *Geological Society, London, Engineering Geology Special Publications* 29(1): **433–56**. doi:10.1144/egsp29.18.

Azhdarpoor, Abooalfazl, Mohammad Hoseini, Samaneh Shahsavani, Narges Shamsedini, and Ehsan Gharehchahi. 2021. “Assessment of Excess Lifetime Cancer Risk and Risk of Lung Cancer Due to Exposure to Radon in a Middle Eastern City in Iran.” *Radiation Medicine and Protection* 2(3): **112–16**. doi:10.1016/j.radmp.2021.07.002.

Catão, Rayssa de Lourdes Carvalho Marinho do Rêgo, Patrícia Hermínio Cunha Feitosa, Andréa Carla Lima Rodrigues, Renata de Albuquerque Cavalcanti Almeida, Dayse Luna Barbosa, and Maria Teresa de Jesus Camelo Guedes. 2022. “Maximum Recommended and Allowable Radon-222 Limits in Water and Air: Systematic Review.” *Research, Society and Development* 11(15): e144111536761. doi:10.33448/rsd-v11i15.36761.

Cevik, U., N. Damla, A. I. Kobya, A. Celik, and A. Kara. 2010a. “Radiation Dose Estimation and Mass Attenuation Coefficients of Marble Used in Turkey.” *Annals of Nuclear Energy* 37(12): **1705–11**. doi:10.1016/j

.anucene.2010.07.011.

Cevik, U., N. Damla, A. I. Kobya, A. Celik, and A. Kara. 2010b. "Radiation Dose Estimation and Mass Attenuation Coefficients of Marble Used in Turkey." *Annals of Nuclear Energy* 37(12): **1705–11**. doi:10.1016/j.anucene.2010.07.011.

Cucoş, Alexandra, Tiberius Dicu, Mircea Moldovan, Gabriel Dobrei, Ancuţa Ţenter, Ştefan Florică, Alexandru Lupulescu, et al. 2025. "A Comparative Analysis of Indoor Radon Activity Concentrations in Romanian Houses and Educational Institutions." *Heliyon* 11(4). doi:10.1016/j.heliyon.2025.e42659.

Dadashpoor, Somayeh, Parvin Nassiri, Alireza Mirzahosseini, Nabiollah Mansouri, and Zahra Azizi. 2025. "Assessment of Carcinogenic Risk from Indoor Radon Exposure Influenced by Geological Structures in the Mountains of Southern Caspian Sea." *Scientific Reports* 15(1): **1–9**. doi:10.1038/s41598-025-98538-3.

Darby, S, D Hill, A Auvinen, H Baysson, F Bochicchio, H Deo, R Falk, et al. 2004. "Radon in Homes and Risk of Lung Cancer: Collaborative Analysis of Individual Data from 13 European Case-Control Studies." 63(December): **4–6**. doi:10.1136/bmj.38308.477650.63.

Degu Belete, Guadie, and Yetsedaw Alemu Anteneh. 2021. "General Overview of Radon Studies in Health Hazard Perspectives." *Journal of Oncology* 2021. doi:10.1155/2021/6659795.

e Silva, Camila Rodrigues, and Emmanoel Vieira Silva-Filho. 2020. "Radon Concentration and Radiation Exposure Levels in Workplace Buildings of Downtown Rio de Janeiro City, SE, Brazil." *Journal of Radioanalytical and*

Nuclear Chemistry 326(3): **1709–17**. doi:10.1007/s10967-020-07463-4.

Elsesmita, Sabrina Ermayanti, and Dewi Wahyu Fitrina. 2022. “Effect of Radon and Lung Cancer Risk: A Narrative Literature Review.” *Bioscientia Medicina : Journal of Biomedicine and Translational Research* 6(15): **2691–98**. doi:10.37275/bsm.v6i15.669.

Elzain, Abd Elmoniem A. 2023. “Assessment of Environmental Health Risks Due to Indoor Radon Levels inside Workplaces in Sudan.” *International Journal of Environmental Analytical Chemistry* 103(6): **1394–1410**. doi:10.1080/03067319.2021.1873317.

Farkas, Árpád. 2020. “Simulation of the Effect of Mucociliary Clearance on the Bronchial Distribution of Inhaled Radon Progenies and Related Cellular Damage Using a New Deposition and Clearance Model for the Lung.” *Radiation and Environmental Biophysics* 59(4): **651–61**. doi:10.1007/s00411-020-00868-5.

Grzywa-Celińska, Anna, Adam Krusiński, Jadwiga Mazur, Katarzyna Szewczyk, and Krzysztof Kozak. 2020. “Radon—the Element of Risk. The Impact of Radon Exposure on Human Health.” *Toxics* 8(4): **1–20**. doi:10.3390/toxics8040120.

Hansen, Violeta, Dorthe Petersen, Jens Søgaard-Hansen, Frank Farsø Rigét, Anders Mosbech, Daniel Spelling Clausen, Gert Mulvad, and Tryggve Rönnqvist. 2023. “Indoor Radon Survey in Greenland and Dose Assessment.” *Journal of Environmental Radioactivity* 257(April 2022). doi:10.1016/j.jenvrad.2022.107080.

ICRP. 2007. “ICRP PUBLICATION 103 The 2007 Recommendations of the

International Commission on Radiological Protection.” *Radiation Physics and Chemistry* 188(24): 1–337. www.mdpi.com/journal/ diagnostics%0Ahttp://www-pub.iaea.org/MTCD/publications/PDF/Pub1609_web.pdf%5Cnhttp://www.vomfi.univ.kiev.ua/assets/files/IAEA/Pub1462_web.pdf%0Ahttp://www.ncbi.nlm.nih.gov/pubmed/16168243.

Kanda, Tripti, Rupanshee Srivastava, Nidhi Singh, and Sadhana Yadav. 2022. Advances in Agriculture and Allied Technologies *Advances in Agriculture and Allied Technologies*. doi:10.22271/ed.book.1919.

Karmaker, Nanda, Kazi M Maraz, Farhana Islam, Marjanul Haque, and M Z I Mollah. 2021. “Fundamental Characteristics and Application of Radiation.”

Kellenbenz, Kyle R., and Kabindra M. Shakya. 2021. “Spatial and Temporal Variations in Indoor Radon Concentrations in Pennsylvania, USA from 1988 to 2018.” *Journal of Environmental Radioactivity* 233(January): 106594. doi:10.1016/j.jenvrad.2021.106594.

Kendall, Gerry M., and T. J. Smith. 2002. “Doses to Organs and Tissues from Radon and Its Decay Products.” *Journal of Radiological Protection* 22(4): 389–406. doi:10.1088/0952-4746/22/4/304.

Kpordzro, R., J. K. Gbadago, A. B. Andam, O. K. Adukpo, F. Otoo, I. Opoku-Ntim, M. Abubakar, and E. Amoatey. 2022. “Assessment of Seasonal Radon Concentration in Dwellings and Soils in Selected Areas in Ga East, Greater Accra Region of Ghana.” *Journal of Environmental and Public Health* 2022. doi:10.1155/2022/6600919.

Lin, Chun Chih, Shih Jung Lin, Pei Ying Li, Moon Sing Lee, and Chien Yi Ting.

2024. “Radon Levels and Dose Assessment at the Basement Workplaces of Hospitals in Different Regions of Taiwan.” *Radiation Physics and Chemistry* 218: 111530. doi:10.1016/j.radphyschem.2024.111530.

Lorenzo-González, María, María Torres-Durán, Raquel Barbosa-Lorenzo, Mariano Provencio-Pulla, Juan Miguel Barros-Dios, and Alberto Ruano-Ravina. 2019. “Radon Exposure: A Major Cause of Lung Cancer.” *Expert Review of Respiratory Medicine* 13(9): **839–50**. doi:10.1080/ 17476348.2019.1645599.

Machraoui, Sonia, Salam Labidi, and Ahmed Azbouche. 2024. “Assessment of Radon Levels in Indoor Workplaces in Tunisia and Associated Radiological Risks.” *International Journal of Environmental Analytical Chemistry* 00(00): **1–17**. doi:10.1080/03067319.2024.2382371.

Maier, Andreas, Julia Wiedemann, Felicitas Rapp, Franziska Papenfuß, Franz Rödel, Stephanie Hehlgans, Udo S Gaipl, et al. 2021. “Molecular Sciences Radon Exposure-Therapeutic Effect and Cancer Risk.” *Molecular Sciences* 22(316): 1–39. https://doi.org/10.3390/ijms22010316.

Matovu, Joseph K.B., Stephen N. Kabwama, Tonny Ssekamatte, John Ssenkusu, and Rhoda K. Wanyenze. 2021. “COVID-19 Awareness, Adoption of COVID-19 Preventive Measures, and Effects of COVID-19 Lockdown Among Adolescent Boys and Young Men in Kampala, Uganda.” *Journal of Community Health* 46(4): **842–53**. doi:10.1007/s10900-021-00961-w.

Mbida Mbembe, Serge, Bertrand Akamba Mbembe, André Manga, Patrice Ele Abiama, Saidou, Philippe Ondo Meye, Pierre Owono Ateba, and Germain Hubert Ben–Bolie. 2023. “Indoor Radon, External Dose Rate and

Assessment of Lung Cancer Risk in Dwellings: The Case of Ebolowa Town, Southern Cameroon.” *International Journal of Environmental Analytical Chemistry* 103(17): **5957–73**. doi:10.1080/03067319.2021.1946684.

Muhammad, Abdu Nasiru, Aznan Fazli Ismail, and Nuraddeen Nasiru Garba. 2022. “Annual Effective Dose Associated with Radioactivity in Drinking Water from Tin Mining Areas in North-Western Nigeria.” *Journal of Radiation Research and Applied Sciences* 15(3): 96–102. doi:10.1016/J.JRRAS.2022.06.008.

Mukwaya, Paul Isolo, Judith Mbabazi, and Henrik Ernstson. 2025. *Kampala : City Report*. doi:10.13140/RG.2.2.31751.92323.

Obid, Raad, and Hayder Hamza. 2011. “Natural Occurring Radionuclide Materials.” *Radioisotopes - Applications in Physical Sciences* (October 2011). doi:10.5772/20562.

Pant, Preeti, Tushar Kandari, Mukesh Prasad, and R. C. Ramola. 2016. “A Comparative Study of Diurnal Variation of Radon and Thoron Concentrations in Indoor Environment.” *Radiation Protection Dosimetry* 171(2): **212–16.** doi:10.1093/rpd/ncw061.

Pantelić, Gordana, Igor Čeliković, Miloš Živanović, Ivana Vukanac, Jelena Krneta Nikolić, Giorgia Cinelli, and Valeria Gruber. 2019. “Qualitative Overview of Indoor Radon Surveys in Europe.” *Journal of Environmental Radioactivity* 204(April): **163–74**. doi:10.1016/j.jenvrad.2019.04.010.

Papenfuß, Franziska, Andreas Maier, Claudia Fournier, Gerhard Kraft, and Thomas Friedrich. 2022. “In-Vivo Dose Determination in a Human after Radon Exposure: Proof of Principle.” *Radiation and Environmental*

Biophysics 61(2): **279–92**. doi:10.1007/s00411-022-00972-8.

Rahman, S. U., M. Rafique, Matiullah, and J. Anwar. 2010. "Radon Measurement Studies in Workplace Buildings of the Rawalpindi Region and Islamabad Capital Area, Pakistan." *Building and Environment* 45(2): **421–26**. doi:10.1016/j.buildenv.2009.06.019.

Riudavets, Mariona, Marta Garcia de Herreros, Benjamin Besse, and Laura Mezquita. 2022. "Radon and Lung Cancer: Current Trends and Future Perspectives." *Cancers* 14(13): **1–17**. doi:10.3390/cancers14133142.

Shahbazi-Gahrouei, Daryoush, Samaneh Setayandeh, and Mehrdad Gholami. 2013. "A Review on Natural Background Radiation." *Advanced Biomedical Research* 2(1): 65. doi:10.4103/2277-9175.115821.

Teiri, Hakimeh, Shahrokh Nazmara, Ali Abdolahnejad, Yaghoub Hajizadeh, and Mohammad Mehdi Amin. 2021. "Indoor Radon Measurement in Buildings of a University Campus in Central Iran and Estimation of Its Effective Dose and Health Risk Assessment." *Journal of Environmental Health Science and Engineering* 19(2): **1643–52**. doi:10.1007/s40201-021-00720-y.

Tezcan, F., S. Aközcan, and S. Özden. 2023. "Indoor Radon (222Rn) Measurements and Assessment of Human Risk in the Dwellings of Edirne (Türkiye)." *Journal of Radioanalytical and Nuclear Chemistry* 332(11): **4629–40**. doi:10.1007/s10967-023-08918-0.

Trassierra, C. Vargas, L. Stabile, F. Cardellini, L. Morawska, and G. Buonanno. 2016. "Effect of Indoor-Generated Airborne Particles on Radon Progeny Dynamics." *Journal of Hazardous Materials* 314: **155–63**. doi:10.1016/j.jhazmat.2016.04.051.

Tsapalov, Andrey, and Konstantin Kovler. 2021. “Studying Temporal Variations of Indoor Radon as a Vital Step towards Rational and Harmonized International Regulation.” *Environmental Challenges* 4(July): 100204. doi:10.1016/j.envc.2021.100204.

Vimercati, Luigi, Fulvio Fucilli, Domenica Cavone, Luigi De Maria, Francesco Birtolo, Giovanni Maria Ferri, Leonardo Soleo, and Piero Lovreglio. 2018. “Radon Levels in Indoor Environments of the University Hospital in Bari-Apulia Region Southern Italy.” *International Journal of Environmental Research and Public Health* 15(4). doi:10.3390/ijerph15040694.

Wang, Hao, Lei Zhang, Peng Gao, and Qiuju Guo. 2022. “A Pilot Survey on Indoor Radon Concentration in Beijing.” *Radiation Medicine and Protection* 3(1): **22–25**. doi:10.1016/j.radmp.2022.01.003.

Yousif, Jafer Abdulameer, and Ali M Alsahlany. 2022. “Electromagnetic Radiation Effects on The Human Tissues.” *NeuroQuantology* 20(10): **8130–46**. doi:10.14704/nq.2022.20.10.NQ55797.

APPENDIX: RAW DATA

APPENDIX A: Description of the investigated rooms of the occupational buildings and dwellings

Table A 1: Details about the rooms studied in the work buildings.

Site	Location	Altitude	Level	Building and covering materials of rooms
CT-1	N0° 19.042' E32° 34.424'	1165 m	B	Floor covered with ceramics (tiles), painted concrete walls and ceiling, no windows and 1 door, having 1 fan.
			G	Floor covered with ceramics (tiles), painted concrete walls and ceiling, 1 door, no windows and no other ventilation system.
			F1	Floor covered with ceramics (tiles), painted concrete walls and ceiling, 1 door, no windows and no other ventilation system.
CT-2	N0° 18.778' E32° 34.915'	1185 m	B	Floor covered with ceramics (tiles), concrete walls covered with plywood and painted concrete ceiling, 1 door, no windows and any other ventilation.
			G	Tiled floor covered with a carpet, painted concrete walls and ceiling, 1 door and 1 window with no other ventilation.
			F1	Floor covered with ceramics (tiles), painted concrete walls and ceiling, 1 door and 2 windows without other ventilation.
NK-1	N0° 20.975' E32° 37.643'	1221 m	G	Painted concrete ceiling and walls, with a concrete floor, 1 door, 2 windows and other ventilation.
			F1	Painted concrete ceiling and walls, with a concrete floor, 1 door, 2 windows and other ventilation.
			F2	Concrete floor covered with carpet, painted concrete walls and ceiling,

				1 door, 2 windows and other ventilation.
			B	Painted concrete ceiling and walls, with a concrete floor, 1 door, no windows and other ventilation.
NK-2		1186 m	G	Concrete floor, painted concrete walls and ceiling, 1 door and 2 windows and no other ventilation.
	N0° 20.944' E32° 35.532'		F1	Painted concrete ceiling and walls, with a concrete floor, 1 door and 2 windows without other ventilation.
			B	Painted concrete ceiling and walls, with a concrete floor, 1 door, no windows and other ventilation.
MK-1		1208 m	G	Floor covered with ceramics (tiles), painted concrete walls and ceiling, 1 door and 1 window with no other ventilation.
	N0° 18.113' E32° 35.140'		F1	Floor covered with ceramics (tiles), painted concrete walls and ceiling, 1 door, with 1 window and no other ventilation.
			B	Concrete floor, painted concrete walls and ceiling, 1 door, no windows and other ventilation.
MK-2		1165 m	G	Floor covered with ceramics (tiles), painted concrete walls and ceiling, 1 door, no windows and other ventilation.
	N0° 15.618' E32° 36.064'		F1	Floor covered with ceramics (tiles), painted concrete walls and ceiling, 1 door, no windows and other ventilation.
			G	Concrete floor, painted concrete walls and ceiling, 2 doors, no windows and other ventilation.
RB-1		1206 m	F1	Floor covered with ceramics (tiles), walls covered with wallpapers and ceiling covered with paint, 1 door, with 1 window and no other ventilation.
	N0° 19.683' E32° 33.893'		F2	Floor covered with ceramics (tiles), walls covered with wallpapers and ceiling covered with paint, 1 door, with 1 window and no other ventilation.

			G	Concrete floor, painted concrete walls and ceiling, 1 door, no windows and other ventilation.
RB-2		1259 m	F1	Floor covered with ceramics (tiles), painted concrete walls and ceiling, 1 door, no windows and other ventilation.
	N0° 18.770' E32° 33.486'		F2	Floor covered with ceramics (tiles), painted concrete walls and ceiling, 1 door, no windows and other ventilation.
			G	Floor covered with ceramics (tiles), painted concrete walls and ceiling, 1 door, with 1 window and other ventilation.
KW-1		1201 m	F1	Floor covered with ceramics (tiles), painted concrete walls and ceiling, 1 door, with 1 window and other ventilation.
	N0° 22.744' E32° 33.455'		F2	Floor covered with ceramics (tiles), painted concrete walls and ceiling, 1 door, with 1 window and other ventilation.
			B	Concrete floor, painted concrete walls and ceiling, 1 door, no windows and other ventilation.
KW-2		1227 m	G	Floor covered with ceramics (tiles), painted concrete walls and ceiling, 1 door, with 1 window and 1 fan.
	N0° 20.509' E32° 35.026'		F1	Floor covered with ceramics (tiles), painted concrete walls and ceiling, 1 door, with windows and other ventilation.

Table A 2: Details about the rooms studied in the dwellings.

Site	Location	Altitude	Room	Description
KW-1	N0° 21.573' E32° 35.311'	1198 m	Sitting	Floor covered with concrete cement, painted walls and ceiling, 1 window and 1inlet door with rovers as the ventilation system.
			Bedroom	Floor covered with concrete cement, painted walls and ceiling, 1 window and 1 door to the sitting room.
KW-2	N0° 21.764' E32° 33.073'	1203 m	Sitting	Floor covered with tiles, painted walls and ceiling, 1 window and 1 door with rovers as the ventilation system.
			Bedroom	Floor covered with tiles, painted walls and ceiling, 2 windows with rovers and 1 door with the ventilation system.
NK-1	N0° 18.881' E32° 39.126'	1165 m	Sitting	Floor covered with concrete cement, painted walls and ceiling, 1 door and 1 window with 2 ventilators.
			Bedroom	Floor covered with concrete cement, painted walls and ceiling, 1 door and 1 window with 2 ventilators.
NK-2	N0° 20.564' E32° 38.023'	1176 m	Sitting	Floor covered with concrete cement, painted walls and ceiling, 1 window and 1 door and a ventilator.
			Bedroom	The floor is covered with cement, the painted walls and ceiling, 1 window and 1 door and a ventilator.
MK-1	N0° 15.912' E32° 36.310'	1235 m	Sitting	The floor is covered with tiles, walls and ceiling are covered with

				paint, 1 window and 1 door with rovers as the ventilation system in the sitting room.
			Bedroom	Floor covered with tiles, painted walls and ceiling, 1 window and 1 door with rovers as the ventilation system.
MK-2	N0° 15.507' E32° 38.047'	1170 m	Sitting	Floor covered with concrete cement, painted walls and ceiling, 1 window and 1 door and ventilators.
			Bedroom	Floor covered with tiles, painted walls and ceiling, 1 window and 1 door with ventilators.
CT-1	N0° 20.521' E32° 35.415'	1223 m	Sitting	Floor covered with tiles, painted walls and ceiling, 1 window and 1 door with rovers as the ventilation system.
			Bedroom	Floor covered with tiles, painted walls and ceiling, 1 window and 1 door with rovers as the ventilation system.
CT-2	N0° 18.271' E32° 34.403'	1195 m	Sitting	Floor covered with tiles, painted walls and ceiling, 1 window and 1 door with rovers as the ventilation system.
			Bedroom	Floor covered with tiles, painted walls and ceiling, 2 windows and 1 door with rovers as the ventilation system.
MK-1	N0° 19.475' E32° 32.627'	1202 m	Sitting	The floor is covered with tiles cement, painted walls and ceiling, 1 door with rovers as the ventilation system.
			Bedroom	Floor covered with tiles, painted concrete walls and ceiling, 1 door

				with rovers as the ventilation system.
			Sitting	Floor covered with tiles, painted concrete walls and ceiling, 1 window and 1 door with rovers as the ventilation system.
MK-2	N0° 18.144' E32° 33.754'	1207 m	Bedroom	Floor covered with tiles, painted concrete walls and ceiling, 1 window and 1 door with rovers as the ventilation system.

APPENDIX B: ACTIVITY RADON CONCENTRATION IN INVESTIGATED BUILDINGS

Table B 1: Measured levels of ^{222} Rn in the basement areas of the surveyed buildings.

Time (min)	**CT-1**	**CT-2**	**NK-1**	**MK-1**	**MK-2**	**KW-1**
0	12.6	9.8	54.9	20.2	141	30.1
30	15.1	10.1	49.6	49.9	104.8	24.8
60	27.7	19.7	64.2	60.1	124.4	24.9
90	47.3	45	64.8	14.8	148.7	15.2
120	30.2	9.8	45	29.8	130.5	25.1
150	27.5	10.2	40	25	109.7	9.9
180	49.9	5	54.7	20.1	100.3	39.8
210	20.1	5.2	9.8	20	114.5	4.9
240	22.3	15.1	20	15	89.4	10.2
270	39.7	15	55	10	60	0
300	37.4	25.1	24.9	15	74.9	20.1
330	42.2	10.2	24.8	30.6	50.3	15.1
360	17.3	15	34.7	35.5	54.9	20
390	42.6	40.4	24.9	49.6	54.7	20.2
420	30.2	34.7	24.8	10.3	104.6	9.8
450	25.2	39.5	24.8	25	69.4	10

Table B 2: Measured levels of ^{222} Rn on the ground floors of the surveyed buildings.

Time (min)	CT-1	CT-2	NK-1	NK-2	MK-1	MK-2	RB-1	RB-2	KW-1	KW-2
0	10	10	10.1	52.4	9.9	20.1	25.1	19.9	15.2	49.8
30	39.7	10	14.9	56.9	5	79.3	20	70.2	14.9	55.1
60	10	17.3	14.8	54.1	25.1	90.9	35.2	59.7	20	60.2
90	24.7	22.7	4.9	52.4	15.1	94.4	20.3	44.6	9.8	85.3
120	30	3.9	30	47.1	19.8	69.3	14.8	54.3	9.9	54.9
150	25.1	5	30.1	27.2	9.9	54.6	15	64.9	5	50
180	19.8	7.6	19.7	14.9	4.9	34.8	24.7	70.4	10	70
210	20.1	12.4	5.2	27.3	30.3	49.4	9.8	50.2	0	70.2
240	40	12.7	24.9	27.1	25	54.9	15.3	64.3	9.9	50
270	24.7	2.5	55.1	14.8	29.9	60.6	0	99.9	20.1	59.7
300	9.7	2.5	70.1	17.4	35.1	69.4	5	89.9	9.9	59.7
330	39.8	2.5	19.7	22.4	29.8	74.6	10.1	114.7	15.2	95
360	39.8	2.5	25.2	24.8	19.9	89.3	5	139.7	20.1	74.9
390	24.9	7.5	64.5	24.6	24.7	60.3	10	109.3	9.9	85
420	29.8	12.6	19.8	17.1	24.3	40.2	24.7	130.8	4.9	89.9
450	10.1	7.7	45	17.3	24.7	39.5	20.1	85	14.8	94.6

Table B 3: Measured levels of ^{222} Rn on the first floors of the surveyed buildings.

Time (min)	CT-1	CT-2	NK-1	NK-2	MK-1	MK-2	RB-1	RB-2	KW-1	KW-2
0	5	42.5	5	4.6	4.9	9.8	10	44.6	19.9	24.9
30	14.9	30	10	7.2	24.7	10.1	15.3	19.9	20	20
60	14.9	22.3	20	10	20.2	14.9	10	19.8	20	64.9
90	25.2	19.9	10	24.7	14.7	5	20.3	64.8	9.9	30.1
120	10.2	12.5	15.2	17.2	10	0	20.2	65.1	0	35.3
150	20.1	14.8	9.9	17.3	15.2	9.7	10.2	44.9	9.9	50.1
180	39.8	5	15.1	14.6	0	4.9	20.2	80.1	4.9	85
210	19.9	7.5	20.1	24.8	10	20.2	15	74.6	5.2	24.8
240	29.8	17.4	14.8	16.1	15.2	5.2	15	89.6	5	44.8
270	24.8	9.9	5	11	5	0	0	125	14.8	49.6
300	9.8	5	4.9	4.8	5	15.1	5	94.1	35.2	54.8
330	14.9	10	10.2	17.2	34.6	15.1	0	85	10.3	64.8
360	15.1	17.5	5	17.4	39.9	5	5.2	95.1	0	49.6
390	10	2.5	14.9	17.6	10.1	10.2	0	80.4	15.1	60.4
420	30.3	0	9.9	6.7	15.1	9.9	10.2	120	5	49.7
450	9.9	7.5	9.9	24.7	24.9	15.1	20	85.4	15.5	44.8

Table B 4: Measured levels of ^{222} Rn on the second floors of the surveyed buildings.

Time (min)	RB-1	RB-2	NK-2	KW-2
0	24.8	39.5	10	10
30	4.9	14.7	9.9	39.9
60	10.2	59.7	7.4	44.7
90	4.9	30	17.8	24.9
120	14.8	45.2	14.7	40.3
150	10	65.4	17.1	25
180	9.7	35	5	19.8
210	9.9	54.8	2.4	19.8
240	15.5	95.1	10	40.1
270	14.7	84.6	2.5	24.7
300	10	90.8	7.3	30.2
330	10	69.3	7.4	25.1
360	4.9	93.5	9.9	35
390	9.8	89.6	10.1	44.8
420	5	92.1	5	34.5
450	0	80.1	4.9	55.2

Table B 5: Measured levels of ^{222} Rn in the poorly ventilated storage rooms of NK-1 building.

Time (min)	Ground floor	First floor	Second floor
0	40	44.9	109.6
30	34.9	95.4	189.2
60	115.5	125.2	150.6
90	105.2	199.8	135.4
120	241.5	218.8	149.3
150	139.3	214	134.7
180	194.5	249.4	165.2
210	224.6	274.3	179.1
240	299.4	184.8	99.7
270	210.4	178.6	97.2
300	288.8	145.2	100.3
330	249.9	109.5	109.4
360	304.8	144.8	159.7
390	214.3	169.8	159.6
420	224.7	144.1	129.1
450	228.6	155.2	119.1

APPENDIX C: ACTIVITY RADON CONC IN INVESTIGATED DWELLINGS

Table C 1: Measured levels of ^{222} Rn in the bedrooms of the dwellings.

Time	KW-1	KW-2	NK-1	NK-2	MK-1	MK-2	CT-1	CT-2	RB-1	RB-2
0	20.3	50.3	34.9	60	119.3	20.1	15.3	74.7	15.1	30
30	49.9	30	59.2	89.4	130.3	35	24.6	54.6	14.8	45.1
60	25.1	35.4	65.1	115	170.2	15	25.1	59.7	30.1	55.4
90	39.8	45.4	130.8	64.4	139.5	30.4	4.9	60.2	39.9	55.2
120	30	40	138.6	79.7	144.6	55	9.8	89.5	39.9	24.9
150	29.8	34.7	160.1	55	268.5	74.8	24.8	59.6	29.9	15
180	49.6	30.1	224.3	69.4	204.5	69.7	14.7	39.9	50.1	20
210	65	40.2	220	50	183.4	104.8	19.8	75.9	45.2	25
240	34.9	24.7	249.8	94.7	130.3	90.1	4.9	44.7	85.5	20.3
270	49.8	40.1	250.5	174.7	120.2	100.2	20.2	75.4	65.1	10.1
300	64.5	24.7	280.7	209.8	139.5	54.6	14.9	65.7	79.8	15
330	65.3	34.8	273.6	169.6	144.6	85.2	19.9	44.9	120.6	40
360	39.9	29.7	279.5	153.7	218.5	75.2	15	49.5	145.8	34.7
390	59.9	35	249.7	155.3	204.5	69.7	15.2	44.8	89.9	19.8
420	65.3	34.6	219.4	179.6	183.4	75.1	19.8	84.3	115.3	25.1
450	65.1	40.3	306.2	110.3	209.1	75	30	65.4	119.9	34.8

Table C 2: Measured levels of ^{222} Rn in the sittings of the surveyed dwellings.

Time (min)	KW -1	KW -2	NK-1	NK-2	MK-1	MK-2	CT-1	CT-2	RB-1	RB-2
0	15.1	20.1	95.2	60	89.5	24.9	14.8	9.9	24.8	29.8
30	14.9	20.2	115.9	89.4	89.6	25	4.9	14.9	10.1	40
60	19.9	5	140.6	115	124.7	44.8	4.9	14.9	34.9	15
90	24.9	4.9	189.6	64.4	105.2	49.8	4.9	14.8	20.4	29.9
120	10.2	5	175	79.7	69.9	34.8	20.1	29.7	50.3	24.9
150	15	25	219.3	55	94.8	84.7	10	24.7	35	55.2
180	25.1	4.9	199.4	69.4	110.4	79.9	9.9	74.8	44.8	25.1
210	39.7	20.1	215	50	80.6	84.1	15	20.1	40.6	25.1
240	35	20.2	244	94.7	85.4	59.5	14.8	35	44.8	59.7
270	35.1	19.9	234.6	174.7	74.9	64.6	14.9	15.2	49.6	65.1
300	30.1	15.2	183.8	209.8	114.5	89.7	10.3	29.8	64.8	44.7
330	44.8	40	239.3	169.6	79.7	50.5	19.9	9.9	70.5	40.2
360	24.9	29.7	169.4	153.7	84.8	49.6	9.9	29.7	59.6	59.4
390	40	24.6	174.3	155.3	139.3	39.9	14.9	34.7	49.9	54.5
420	19.7	40.2	175	179.6	129.4	34.9	10.2	30.2	39.7	49.7
450	20	24.8	109.6	110.3	144.8	44.7	25.2	39.7	54.7	49.5

APPENDIX D: RADIOLOGICAL RISK ASSESSMENT

Table D 1: Annual radiation effective dose, ERD, ELCR and LCC to workers

N/S	Division	Site	Floor	ED ± Er (mSv/year)	ERD ± Er (mSv/year)	ELCR ± Er ($\times 10^{-4}$)	LCC ± Er (million^{-1})
1	CENTRAL	CT-1	B	0.32 ± 0.03	0.74 ± 0.07	12.32 ± 1.16	5.76 ± 0.54
			G	0.26 ± 0.03	0.62 ± 0.07	10.01 ± 1.16	4.68 ± 0.54
			F1	0.19 ± 0.02	0.46 ± 0.05	7.32 ± 0.77	3.42 ± 0.36
2		CT-2	B	0.20 ± 0.03	0.48 ± 0.07	7.70 ± 1.16	3.60 ± 0.54
			G	0.09 ± 0.02	0.22 ± 0.05	3.47 ± 0.77	1.62 ± 0.36
			F1	0.15 ± 0.03	0.36 ± 0.07	5.78 ± 1.16	2.70 ± 0.54
3	NAKAWA	NK-2	G	0.32 ± 0.04	0.77 ± 0.10	12.32 ± 1.54	5.76 ± 0.72
			F1	0.16 ± 0.01	0.38 ± 0.02	6.16 ± 0.39	2.88 ± 0.18
			F2	0.09 ± 0.01	0.22 ± 0.02	3.47 ± 0.39	1.62 ± 0.18
4		NK-1	B	0.40 ± 0.04	0.96 ± 0.10	15.40 ± 1.54	7.20 ± 0.72
			G	0.30 ± 0.05	0.72 ± 0.12	11.55 ± 1.93	5.40 ± 0.90
			F1	0.12 ± 0.01	0.29 ± 0.02	4.62 ± 0.39	2.16 ± 0.18
5	MAKINDYE	MK-1	B	0.28 ± 0.04	0.67 ± 0.10	10.78 ± 1.54	5.04 ± 0.72
			G	0.22 ± 0.02	0.53 ± 0.05	8.47 ± 0.77	3.96 ± 0.36
			F1	0.16 ± 0.03	0.38 ± 0.07	6.16 ± 1.16	2.88 ± 0.54
6		MK-2	B	1.00 ± 0.08	2.40 ± 0.19	38.50 ± 3.08	18.00 ± 1.44
			G	0.64 ± 0.06	1.54 ± 0.14	24.64 ± 2.31	11.52 ± 1.08
			F1	0.10 ± 0.01	0.24 ± 0.02	3.85 ± 0.39	1.80 ± 0.18
			G	0.17 ± 0.02	0.41 ± 0.05	6.55 ± 0.77	3.06 ± 0.36

7	RUBAGA	RB-1	F1	0.11 ± 0.02	0.26 ± 0.05	4.24 ± 0.77	1.98 ± 0.36
			F2	0.10 ± 0.03	0.24 ± 0.07	3.85 ± 1.16	1.80 ± 0.54
8		RB-2	G	0.82 ± 0.09	1.97 ± 0.22	31.57 ± 3.47	14.76 ± 1.62
			F1	0.77 ± 0.08	1.85 ± 0.19	29.65 ± 3.08	13.86 ± 1.44
			F2	0.68 ± 0.06	1.63 ± 0.14	26.18 ± 2.31	12.24 ± 1.08
9	KAWEMPE	KW-2	G	0.72 ± 0.04	1.73 ± 0.10	27.72 ± 1.54	12.96 ± 0.72
			F1	0.49 ± 0.04	1.18 ± 0.10	18.87 ± 1.54	8.82 ± 0.72
			F2	0.33 ± 0.08	0.79 ± 0.19	12.71 ± 3.08	5.94 ± 1.44
10		KW-1	B	0.18 ± 0.03	0.43 ± 0.07	6.93 ± 1.16	3.24 ± 0.54
			G	0.12 ± 0.01	0.29 ± 0.02	4.62 ± 0.39	2.16 ± 0.18
			F1	0.12 ± 0.02	0.29 ± 0.05	4.62 ± 0.77	2.16 ± 0.36
			STORAGE ROOMS WITH POOR VENTILATION				
	NAKAWA	NK-1	G	2.03 ± 0.22	4.87 ± 0.53	78.16 ± 8.47	36.54 ± 3.96
			F1	1.73 ± 0.15	4.15 ± 0.36	66.61 ± 5.78	31.14 ± 2.70
			F2	1.42 ± 0.08	3.41 ± 0.19	54.67 ± 3.08	25.56 ± 1.44

Table D 2: Annual radiation effective dose, ERD, ELCR and LCC to dweller

N/S	DIVISION	Site	ED ± Er (mSv/year)	ERD ± Er (mSv/year)	ELCR ± Er ($\times 10^{-4}$)	LCC ± Er (million^{-1})
1	CENTRAL	CT-1	0.16 ± 0.02	0.38 ± 0.06	6.16 ± 0.77	2.88 ± 0.36
2		CT-2	0.46 ± 0.18	1.11 ± 0.44	17.71 ± 6.93	8.28 ± 3.24
3	NAKAWA	NK-1	1.96 ± 0.09	4.70 ± 0.20	75.46 ± 3.47	35.28 ± 1.62
4		NK-2	1.10 ± 0.09	2.64 ± 0.21	42.35 ± 3.47	19.80 ± 1.62
5	MAKINDYE	MK-1	1.41 ± 0.42	3.39 ± 1.00	54.29 ± 16.17	25.38 ± 7.56
6		MK-2	0.62 ± 0.06	1.48 ± 0.13	23.87 ± 2.31	11.16 ± 1.08
7	RUBAGA	RB-1	0.72 ± 0.18	1.73 ± 0.43	27.72 ± 6.93	12.96 ± 3.24
8		RB-2	0.36 ± 0.07	0.87 ± 0.17	13.86 ± 2.70	6.48 ± 1.26
9	KAWEMPE	KW-1	0.38 ± 0.11	0.91 ± 0.26	14.63 ± 4.24	6.84 ± 1.98
10		KW-2	0.29 ± 0.08	0.69 ± 0.19	11.17 ± 3.08	5.22 ± 1.44